

# **Application of Chemical Heat Pumps for Temperature Amplification in Nuclear Hybrid Energy Systems for Synthetic Transportation Fuel Production**

Piyush Sabharwall  
Daniel Wendt  
Vivek P. Utgikar

October 2013



The INL is a U.S. Department of Energy National Laboratory  
operated by Battelle Energy Alliance

#### **DISCLAIMER**

This information was prepared as an account of work sponsored by an agency of the U.S. Government. Neither the U.S. Government nor any agency thereof, nor any of their employees, makes any warranty, expressed or implied, or assumes any legal liability or responsibility for the accuracy, completeness, or usefulness, of any information, apparatus, product, or process disclosed, or represents that its use would not infringe privately owned rights. References herein to any specific commercial product, process, or service by trade name, trade mark, manufacturer, or otherwise, does not necessarily constitute or imply its endorsement, recommendation, or favoring by the U.S. Government or any agency thereof. The views and opinions of authors expressed herein do not necessarily state or reflect those of the U.S. Government or any agency thereof.

# **Application of Chemical Heat Pumps for Temperature Amplification in Nuclear Hybrid Energy Systems for Synthetic Transportation Fuel Production**

**Piyush Sabharwall and Daniel Wendt, INL  
Vivek P. Utgikar, Dept of Chemical and Material Science Engineering,  
University of Idaho**

**October 2013**

**Idaho National Laboratory  
Originating Organization  
Idaho Falls, Idaho 83415**

**<http://www.inl.gov>**

**Prepared for the  
U.S. Department of Energy  
Office of Nuclear Energy  
Under DOE Idaho Operations Office  
Contract DE-AC07-05ID14517**



## SUMMARY

A chemical heat pump (ChHP) system is a key component of the nuclear hybrid energy systems that can amplify the temperature of conventional Light Water Reactors (LWRs). The high-temperature heat obtained can be utilized for producing synthetic transportation fuels. The overall goal of this project was to analyze and develop a ChHP that can perform the required temperature amplification to deliver high-temperature heat necessary for the above application, and thus contribute significantly to energy security and affordability of the nation.

The activities conducted include a literature survey of ChHPs, identification of candidate ChHP and suitable biomass/carbon resource for the synthesis of the transportation fuels, thermodynamic analysis of the system, and definition of the systems for further thermodynamic, economic, and environmental analysis. The literature search indicated that reversible hydration/dehydration cycle based on  $\text{Ca(OH)}_2/\text{CaO}$  has potential to provide the desired temperature amplification. Preliminary thermodynamic efficiency analysis was conducted for this ChHP. The literature search also indicated poplar trees to be an attractive biomass material for conversion into transportation fuel. It is recommended that further research be undertaken on this ChHP to complete the thermodynamic analysis and determine the feasibility through bench- and pilot-scale experimentation.



## CONTENTS

SUMMARY .....	iii
ACRONYMS .....	vii
1. INTRODUCTION .....	1
2. TEMPERATURE AMPLIFICATION .....	2
2.1 Technologies, Principles, and Operating Conditions .....	2
2.1.1 Mechanical Heat Pumps .....	2
2.2 Vapor Absorption Heat Pumps .....	3
2.2.1 Solid State Heat Pumps .....	3
2.2.2 Chemical Heat Pumps .....	3
3. SCREENING CRITERIA AND IDENTIFICATION OF CANDIDATE TEMPERATURE AMPLIFICATION TECHNOLOGY .....	6
4. PRINCIPLES OF OPERATION .....	9
4.1 Synthesis/Production/Heat-Release Step .....	9
4.2 Regeneration/Decomposition Step .....	10
5. THERMODYNAMIC ANALYSIS .....	10
5.1 Process Conditions .....	12
5.2 Efficiency Calculations .....	13
5.2.1 Enthalpy of reaction .....	14
5.2.2 Temperature Level .....	14
6. ENVIRONMENTAL LIFE CYCLE ASSESSMENT .....	15
7. FUTURE WORK AND PATH FORWARD .....	16
8. REFERENCES .....	17
8.1.1 MgO/H <sub>2</sub> O/Mg(OH) <sub>2</sub> chemical heat pumps .....	9
REFERENCES .....	16

## FIGURES

Figure 1. Process heat applications of nuclear reactors. ....	1
Figure 2. Operating principle of chemical heat transformer (pump). ....	4
Figure 3. Classification of ChHPs Systems (Cot-Gores et al. 2012). ....	5
Figure 4. Temperature pressure diagram (Hasatani 1992). ....	8
Figure 5. Schematic of the proposed nuclear reactor-ChHP system for syngas production from biomass. ....	9
Figure 6. Clausius-Clapeyron diagram for chemical heat transformer operation. ....	10

Figure 7. Equilibrium of $\text{Ca(OH)}_2 \leftrightarrow \text{CaO} + \text{H}_2\text{O}$ .....	11
Figure 8. Clausius-Clapeyron diagram for the hydration/dehydration of calcium oxide.....	12
Figure 9. Calcium oxide hydration/dehydration temperature amplification ChHP for upgrading LWR outlet temperature .....	13

## TABLES

Table 1. Thermal efficiency of calcium oxide hydration/dehydration ChHP using heat of reaction values reported in various literature sources.....	14
--	----



## ACRONYMS

ChHP	Chemical Heat Pump
COP	Coefficient of Performance
LCA	Life Cycle Assessment
LWR	Light Water Reactor
NHES	Nuclear Hybrid Energy System
SMR	Small Modular Reactor

# Application of Chemical Heat Pumps for Temperature Amplification in Nuclear Hybrid Energy Systems for Synthetic Transportation Fuel Production

## 1. INTRODUCTION

Nuclear energy is the key to the long-term energy security and sustainability of carbon-free energy future of the nation. Nuclear reactors are ideally suited to provide baseload electric power; however, integration of the nuclear energy in process heat and other non-electric power uses, such as manufacturing synthetic transportation fuels, requires the development of nuclear hybrid energy systems (NHESs). NHESs are ideally suited to enhance the nation's energy security while minimizing emission concerns. The potential applications of nuclear reactors for non-power generation applications are shown below in Figure 1 (Park et al. 2009).

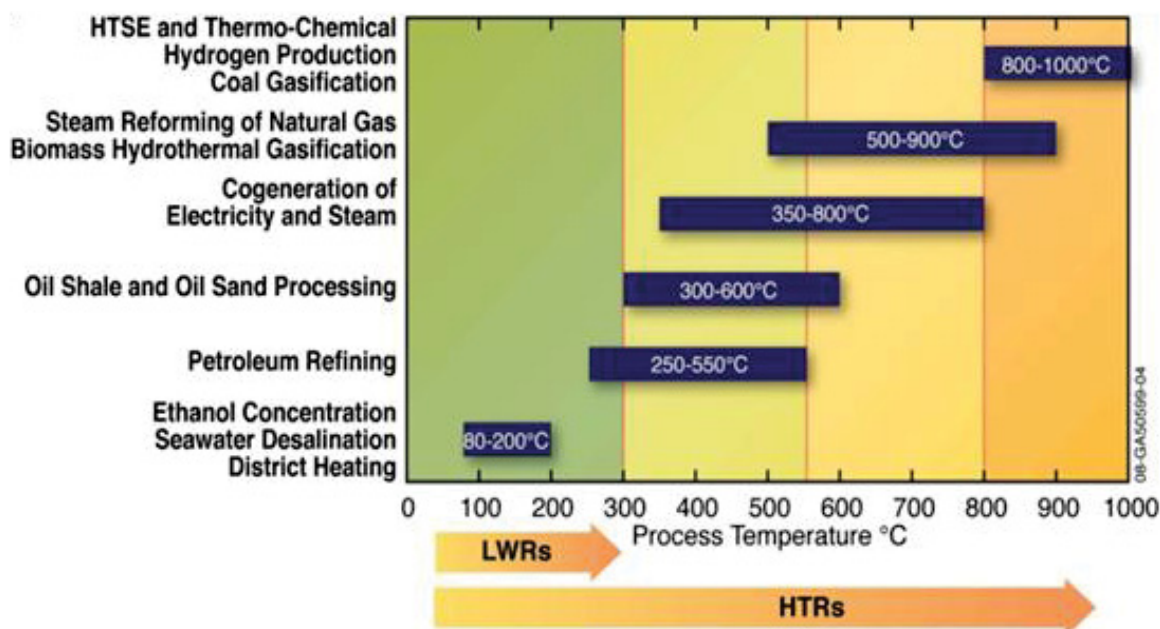


Figure 1. Process heat applications of nuclear reactors.

The first generation NHES will likely be based on conventional light-water reactors (LWRs). Temperature requirements of many of these processes are typically higher than those available from the conventional LWRs, and thermoamplification technologies are essential for the NHESs based on the conventional LWRs. Chemical heat pumps (ChHPs), with their ability for long-term, high-capacity thermal storage with low energy losses (Wongsuwan et al. 2001), are attractive alternatives for achieving this temperature amplification. This research is based on the hypothesis that ChHPs, which use reversible chemical reactions, can be integral components of NHES for upgrading the thermal energy of nuclear reactors.

The following objectives were defined for this research for the development of ChHPs in NHESs:

1. Conduct a literature review, evaluation, and down selection of a candidate ChHP systems that would be applicable to upgrade the thermal energy produced by a small modular (SMR) LWR (nuclear).
2. Complete thermodynamic calculations and preliminary economical feasibility assessments of the candidate ChHP systems.

3. Provided there is justification to proceed, set up a lab-scale test prototype and collect data to verify the thermodynamic and heat transfer mechanisms of the ChHP unit operations.
4. Complete a plant design and economics study to evaluate an integrated system consisting of a nuclear reactor (current LWRs or advanced SMRs based on the LWR design), a ChHP, and a select fuels production plant, such as a biomass-conversion system to produce 10,000 barrels per day of liquid transportation fuel.

## **2. TEMPERATURE AMPLIFICATION**

### **2.1 Technologies, Principles, and Operating Conditions**

Various alternatives for amplifying LWR outlet temperature are briefly described below.

#### **2.1.1 Mechanical Heat Pumps**

##### **2.1.1.1 Vapor Compression (Reverse Rankine Cycle)**

Vapor compression heat pumps utilize the Rankine cycle operating in reverse. Low-temperature heat is supplied to an evaporator, where a working fluid in the liquid phase is vaporized. Mechanical power is used to compress the vapor phase working fluid, increasing the temperature of the vapor to produce a superheated vapor. The superheated vapor is then cooled and condensed, releasing heat at a temperature greater than that input to the evaporator. The liquid then flows through a valve where its pressure is reduced prior to reentering the evaporator. The heat released from the cycle in the condenser may be used for the desired application.

Various working fluids may be utilized in the vapor compression heat pump, depending on the heat source and sink temperatures and desired process characteristics. Supercritical CO<sub>2</sub> heat pump cycles may achieve output temperatures of up to 150°C using waste heat input (Thermea Energiesysteme, 2008).

Open or semi-open systems utilizing mechanical vapor recompression (MVR) and condensation of vapor from industrial processes work with heat-source temperatures from 70-80°C and deliver heat between 110 and 150°C, in some cases up to 200°C (Heat Pump Centre, 2007)

##### **2.1.1.2 Gas Cycle (reverse Brayton cycle)**

The reverse Brayton cycle may also be used for heat pumping applications. In this cycle, the working fluid remains in the gas phase, resulting in use of gas-to-gas heat exchangers and large volumetric flow rates. The absence of a working fluid phase changes results in non-isothermal heat exchange operations, which may decrease process efficiency, depending on the application.

Efficiencies similar to those of conventional vapor compression cycles can be obtained through selection of cycle operating parameters such that the expansion process occurs in the vicinity of the working fluid critical point (Angelino and Invernizzi, 1995).

Known Brayton cycle industrial heat pump applications include low temperature drying (<150°F) and solvent recovery applications (Mills and Chappell, 1985; and Heat Pump Centre, 2007).

##### **2.1.1.3 Stirling Cycle**

Heat pumps based on the Stirling cycle are not widely utilized. Analysis of the cycle indicate several potential advantages, such as high efficiency, with coefficient of performance (COP) approaching that of an equivalent Carnot cycle. Stirling cycles can utilize noncondensable working fluids, such as hydrogen or helium that are not limited by thermal instability (Mills and Chappell 1985). However, no known high-temperature upgrading applications exist at the present time.

### **2.1.2 Vapor Absorption Heat Pumps**

Absorption heat pumps are driven by thermal rather than mechanical or electrical power sources. Sorption heat pumps use the heat of sorption/desorption of a medium to transfer heat between different temperature levels. Absorption heat pumps may utilize multiple stages to increase system efficiency. Ammonia-water and LiBr-water are the two most common absorption heat pump working fluids. Absorption heat pumps typically have lower efficiency than mechanical heat pumps, but have advantageous properties, such as few moving parts and no mechanical or electrical requirements (aside from instrumentation and controls), that make them favorable in certain applications.

Current LiBr-water absorption heat pump systems achieve an output temperature of 100°C and a temperature lift of 65°C (Heat Pump Centre, 2007). Typical LiBr heat transformer temperatures are limited due to corrosion effects. However, a specialized LiBr-water heat transformer configuration using corrosion resistant graphite has been proposed for operation at temperatures up to 230°C (Le Goff et al, 1993). The newest generation of advanced absorption heat pumps are capable of output temperatures up to 260°C (Heat Pump Centre, 2007).

### **2.1.3 Solid State Heat Pumps**

Solid state heat pumps use magnetic or thermoelectric effects to achieve thermal energy transport and conversion processes. Solid state heat pumps require electrical input to achieve temperature transformation. Theoretical analysis of magnetic heat pumps indicate that the process equipment involves few moving parts, cycle efficiencies could approach Carnot limits with heat transfer being the only inherent irreversibility, and the use of a solid working material eliminates compressors, turbines, and pressure containment problems (Mills and Chappell, 1985). Although numerous magnetic heat pump devices have been tested, maximum temperature lifts obtained are on the order of 50K and the application of these devices appears to be best suited toward refrigeration and space heating and cooling applications.

### **2.1.4 Chemical Heat Pumps**

ChHPs are systems that use reversible chemical reactions for energy storage and release. The energy storage step is endothermic, typically a reaction involving breakage of bonds. Thermal energy is stored as the chemical energy of the products. Reversing the reaction results in the formation of the reactants of the first step. Energy is released in this exothermic step. The reverse reaction may be conducted at higher temperature through the manipulation of reaction conditions, resulting in thermoamplification. The chemical heat transformer/pump utilizes a medium-temperature heat source to generate a higher temperature heat output and a lower temperature heat output. The high-temperature heat is output at a temperature level where it may be reused, while the low-temperature heat is rejected. The basic operating principle is illustrated in Figure 2. The principle is based on two distinct operations: adsorption/synthesis/production and desorption/decomposition/regeneration. With a solid/gas dual reactor system, these operations occur in pairs—when the low-temperature reactor is regenerating, the high-temperature reactor is producing, and vice versa.

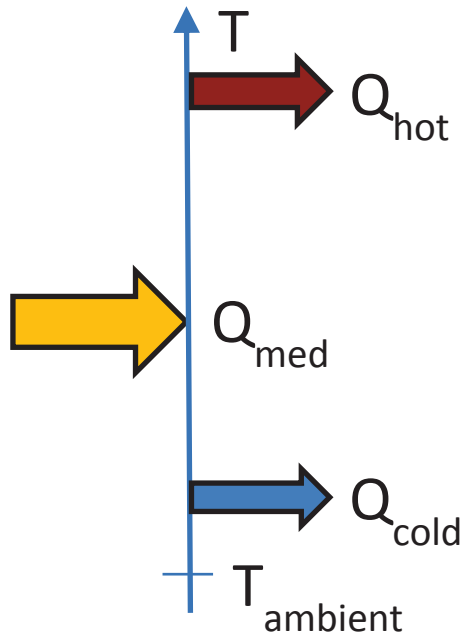
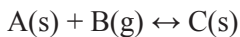


Figure 2. Operating principle of chemical heat transformer (pump).

The general reaction-taking place in the chemical heat pump reactor is of the form:



Where the forward and backward reactions occur at two different temperatures, which allows the upgrading of heat from low to high temperature (Wongsuwan et al. 2001). In this generalized reaction scheme, the forward reaction is endothermic while the reverse reaction is exothermic.

Chemical heat pumps can utilize heat sources, such as LWR heat, directly without requiring conversion of the energy to mechanical and/or electrical power. Direct utilization of the heat stream (in secondary loop; some thermodynamic irreversibility will be associated with the primary loop heat exchange process) eliminates irreversibilities associated with conversion to mechanical and electrical power. The primary source of irreversibility in chemical heat pump operation is the batch operating mode that necessitates reaction heating and cooling (with no temperature upgrading occurring during these steps) between production and regeneration operations. The efficiency of the temperature upgrading ChHPs process can be increased by integrating heat utilization to include operations such as recuperation of residual heat at the end of the production phase for use in preheating the regeneration phase reactor. ChHPs offer a wider range of operating temperature and versatility in comparison with conventional vapor compression or (de) sorption heat pump (Arjmand et al. 2012).

ChHPs covers not only chemical reactions, but also physical sorption processes that can be reversed. An extensive literature exists on the ChHPs, which have been typically used for thermal energy storage, space heating and cooling (including refrigeration), drying, and thermoamplification (Wongsuwan et al. 2001). In general, the ChHPs can be classified into those based on sorption processes and those based on chemical reactions (Cot-Gores et al. 2012). The following figure (Figure 3) summarizes the various inorganic ChHPs systems that have been experimentally investigated. The sorption processes generally involve sorption-desorption of water, ammonia, or hydrogen. ChHPs based on reversible chemical reactions typically involve a hydration/dehydration, carbonation/decarbonation, hydrogenation/dehydrogenation, or redox reaction couple.

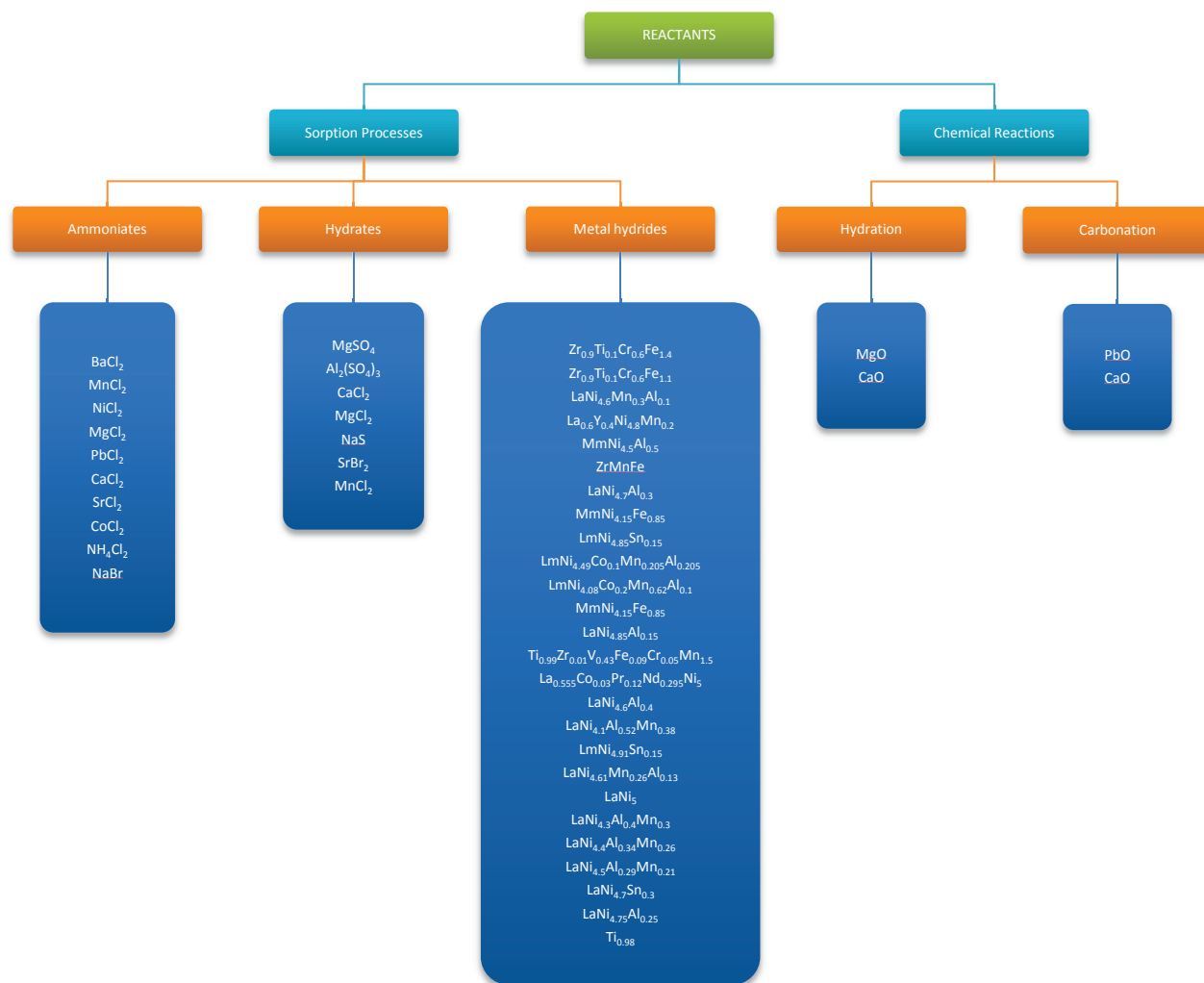
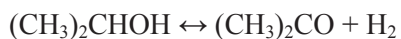


Figure 3. Classification of ChHPs Systems (Cot-Gores et al. 2012).

Isopropanol-acetone is among one the promising organic ChHPs involving the following reversible hydrogenation-dehydrogenation reaction (KlinSoda and Piumsomboon 2007; Spoelstra et al. 2002):

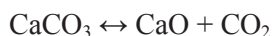
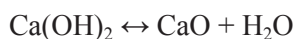


A reversible methanation-steam reforming system is also a possibility for application as a ChHPs. The reaction is (IAEA 1999):



This reaction system has been studied as an energy storage and hydrogen transmission alternative.

The hydration/dehydration and carbonation/decarbonation ChHPs systems are typified through the following reactions involving Ca (Cot-Gores et al. 2012):



The alternative to Ca includes Mg for the hydration/dehydration ChHPs and Pb for carbonation/decarbonation ChHPs. Other examples include chemical-looping reactions, such as metal oxidation/reduction cycles or methane forming/reforming. Sorption processes have been exploited for low temperature applications with maximum output temperatures in the range of 200 to 250°C (Guo and Huai 2012).

Current applications of ChHPs include thermal energy storage, heating and cooling (including refrigeration), and temperature amplification (thermotransformer) (Cot-Gores et al. 2012; Guo and Huai 2012; Olszewski and Saltash 1995; Wongsuwan et al. 2001). Typical uses include refrigeration and air conditioning for ammoniacal system, heat storage, and space heating and cooling for the hydrate and hydride systems (Cot-Gores et al. 2012). Isopropanol-acetone-hydrogen and paraldehyde/acetaldehyde are two of the most commonly investigated organic reaction systems, suitable for low-temperature applications (<200°C) (Guo and Huai, 2012; KlinSoda and Piumsomboon, 2007; Wongsuwan et al. 2001). ChHPs based on these systems will not be able to provide the temperatures necessary for fuel synthesis. Considering the high temperatures required for the decarbonation reactions (>1000 K) in the carbonation/decarbonation ChHPs (Cot-Gores et al. 2012; Ogura et al. 2007), the hydration-based or chemical-looping reaction systems are promising candidates for temperature amplification for LWR-based fuel synthesis. Appendix A provides additional details of some investigations on the ChHPs.

### **3. SCREENING CRITERIA AND IDENTIFICATION OF CANDIDATE TEMPERATURE AMPLIFICATION TECHNOLOGY**

The application of upgrading LWR outlet temperature for providing process heat for thermochemical synthesis of liquid transportation fuels from biomass has a number of specific technology requirements. A list of requirements is provided below:

- Ability to upgrade LWR outlet temperature to levels required for gasification operations (700–850°C)
- Ability to integrate with nuclear hybrid energy systems (tolerant of dynamic or transient operation)
- Any liquid in the system should not freeze at the lowest temperature expected
- High heat of reactions and good reaction kinetics to minimize the storage volume and reactor requirements (McLinden 1980)
- Economic viability, reliability, and operational safety
- Direct utilization of LWR heat: technologies that require mechanical and/or electrical input as the primary energy source will require an additional power conversion operation that is expected to reduce net process efficiency. This requirement eliminates mechanical and solid state (magnetic, thermoelectric, thermoacoustic) heat pumps
- Higher efficiency and better economics than the use of electrical Joule heating to obtain temperature upgrading.

Additionally, NHES operation should provide increased revenues in comparison to entirely electric power generation. The value of chemical products produced using upgraded process heat must outweigh additional process equipment, operations, and maintenance costs in addition to lost/displaced electrical power sales revenues.

Temperature upgrading via mechanical heat pumps is undesirable for LWR coupling due to the requirement that the LWR heat first be converted to mechanical or electrical power, introducing additional operations and thermodynamic losses into the temperature upgrading process. Based on the above selection criteria, chemical heat pumps have been chosen for further evaluation and analysis in the application of upgrading LWR outlet temperature for thermochemical synthesis of liquid transportation fuels. Future detailed analysis to be completed should include an efficiency analysis between ChHP



temperature amplification and a base case in which electrical resistance Joule heating is used to produce process heat at the specified temperature levels.

A limited number of chemical reaction-based ChHPs have been tested by the scientific community. The chemical working pairs that have been tested under various experimental conditions for temperature upgrading applications include  $\text{Mg}(\text{OH})_2/\text{MgO}$ ,  $\text{Ca}(\text{OH})_2/\text{CaO}$ , and  $\text{CaCO}_3/\text{CaO} + \text{PbCO}_3/\text{PbO}$  (Cot-Gores et al. 2012).

The following list summarizes advantages associated with the chemical reaction pairs of  $\text{Ca}(\text{OH})_2/\text{CaO}$  (Hasatani 1992), which is the initial working pair to be analyzed in this research.

- High thermal energy storage density (over 1250 kJ/kg).
- High output temperature (773 K+).
- High reaction rate.
- Good reaction reversibility and durability.
- No toxicity, good reactant corrosion resistance.
- Abundant and low cost CaO resources.
- Hydration/dehydration reaction permits use of evaporator/condenser for low-temperature reactor (simple and low-cost method of collecting, storing, and regenerating mobile phase; eliminates additional packed bed batch mode-only reactor; simplified process control and operation; improved heat and mass transfer characteristics).
- Does not release any contaminating gases (Ogura et al. 1999).

The dehydration-hydration reaction based on CaO is:



The forward endothermic dehydration reaction constitutes the energy storage step, and the energy release occurs during the reverse exothermic hydration reaction. The reaction enthalpy is 104.4 kJ/mol (Schaube et al. 2012). The temperature-pressure diagram is shown in Figure 4 (Hasatani 1992). As shown in Figure 4, the temperature can be amplified up to 1200 K. This ChHP has been investigated for a number of applications, including energy storage and materials drying, and found to offer repeatable thermal output over a number of cycles (Azpiazu et al. 2003; Ogura et al. 2007).



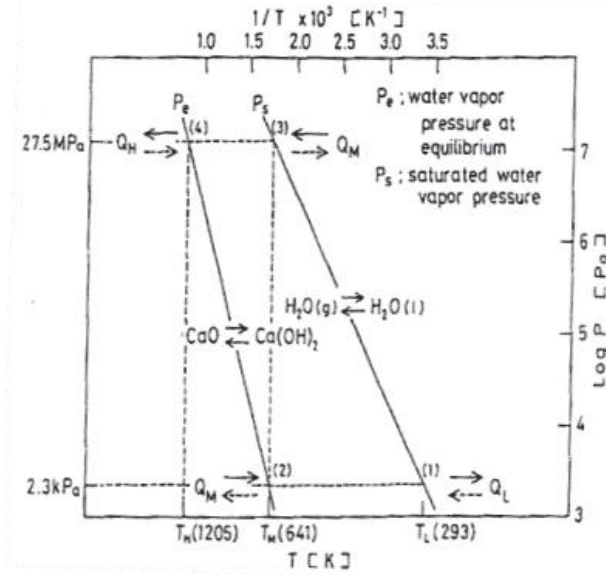


Figure 4. Temperature pressure diagram (Hasatani 1992).

Figure 4 shows that the energy storage step takes place at lower temperatures while the energy release step occurs at higher temperatures (as high as 930°C). Thus, this ChHPs is ideally placed to boost the temperature of the thermal energy of the conventional LWRs for applications such as pyrolysis and fuel synthesis.

Several investigators have examined this system and obtained fundamental information on the thermodynamics and kinetics of the reaction. Some studies have also looked at the reversibility of the reaction system through repeated hydration-dehydration cycles of small (several mg) powdered samples. In spite of these studies, significant uncertainties exist with respect to thermodynamics and kinetics of the reaction, particularly under high partial pressures of water. The issues regarding durability and stability—expansion/contraction and subsequent loss of reactive surface—also need to be addressed for further development of the ChHPs (Cot-Gores et al. 2012). Feasibility of the proposed ChHP's coupling with LWR for fuel synthesis application also needs to be demonstrated. Specifically, the operation of the energy storage step at temperatures corresponding to the LWR outlet temperatures needs to be confirmed.

The integrated system for the a  $\text{CaO}/\text{Ca}(\text{OH})_2$  ChHP could be coupled to a thermochemical biomass conversion process to syngas ( $\text{CO}+\text{H}_2$ ), as shown in Figure 5. The syngas can then be processed via the Fischer-Tropsch (F-T) process to liquid transportation fuels. A nuclear integrated-biomass gasification system will involve the LWR-ChHPs coupling that is able to deliver a high-temperature stream of superheated steam, which can be mixed with ground/pulverized biomass and fed to a biomass reformer for syngas production.

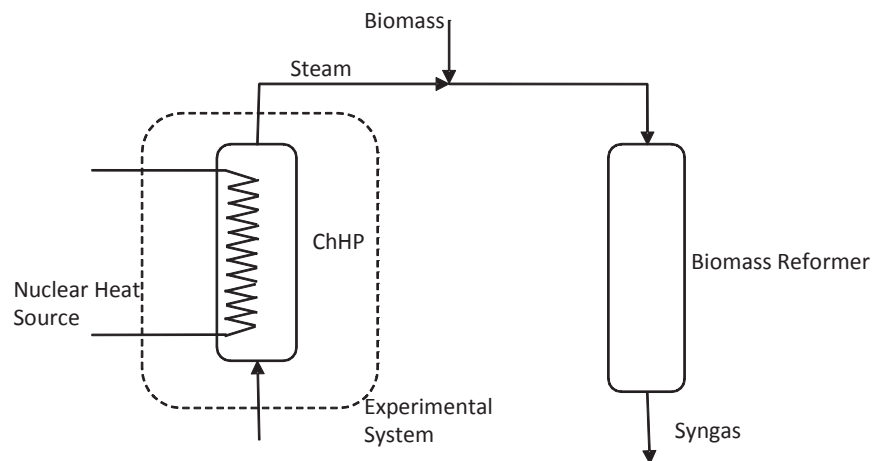


Figure 5. Schematic of the proposed nuclear reactor-ChHP system for syngas production from biomass.

## 4. PRINCIPLES OF OPERATION

A ChHP unit consists of two reactors (or a reactor and an evaporator/condenser) with transport of a mobile phase taking place in a batch process; two or more units each consisting of the high and low-temperature reactors (or reactor and evaporator/condenser) must be implemented to achieve pseudo-steady state operation. The following steps are required for temperature upgrading via hydration/dehydration chemical reaction-based ChHPs.

### 4.1 Synthesis/Production/Heat-Release Step

High-temperature heat is released in the synthesis/production/heat-release chemical heat transformer operation step. In this step, water in the evaporator is vaporized using a medium temperature heat source at supplied at temperature  $T_M$ . As the evaporator temperature increases to  $T_M$ , the vapor pressure of the steam in the evaporator increases according to the equilibrium T-P relation for saturated steam. When the evaporator temperature reaches  $T_M$ , a steam vapor pressure of  $P_H$  exists, at which point the control valve is opened to allow steam at pressure  $P_H$  to enter the synthesis reactor.

As steam flows into the bed and flows/diffuses throughout the reactor bed, exothermic hydration reactions will commence. The P-T relationship for the hydration-dehydration reaction is described by the equilibrium line on the Clausius-Clapeyron diagram (as shown in Figure 6). The reactor bed will heat up to the temperature  $T_H$  corresponding to the steam pressure  $P_H$ , which is a function of the evaporator temperature  $T_M$  as previously described. Energy from the exothermic hydration reaction will be released until the hydration reaction has reached completion or the steam supply is disrupted/discontinued.

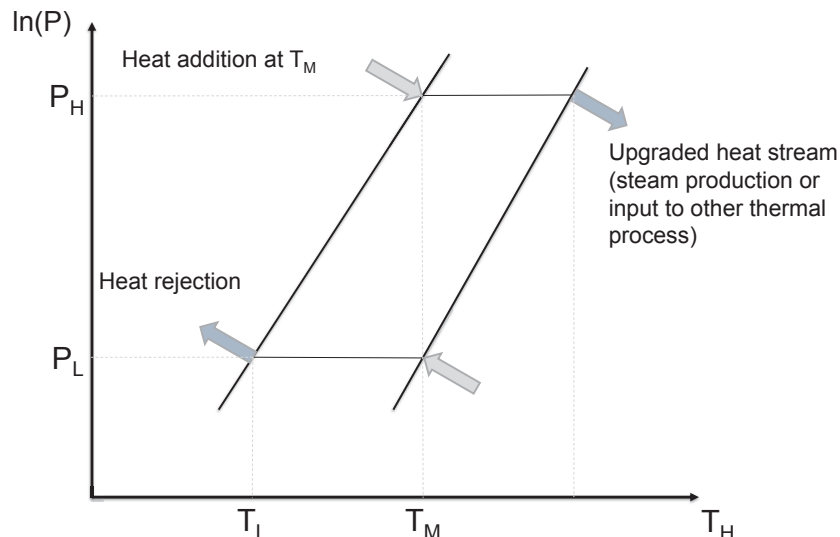


Figure 6. Clausius-Clapeyron diagram for chemical heat transformer operation.

## 4.2 Regeneration/Decomposition Step

Upon completion of the hydration reaction, the reactor bed must be cooled to temperature  $T_M$  for regeneration. For the regeneration operations to occur, the reactor bed pressure must be decreased to a pressure of  $P_L$ . Heat at temperature  $T_M$  is then input to the reactor bed to drive the endothermic dehydration reaction. The water vapor generated by the dehydration reactions flows to the condenser as a result of the pressure differential established as water vapor is condensed in the condenser at a temperature of  $T_L$ . The condenser temperature  $T_L$  determines the system pressure for the regeneration step, as the dew point pressure is a function of temperature for water in the two-phase region.

## 5. THERMODYNAMIC ANALYSIS

ChHPs cycle essentially consists of two parts as explained by Garg et al. (1985), high-temperature cycle (heat engine cycle) and another low-temperature cycle (heat pump cycle). These cycles are coupled to each other and run simultaneously. In ChHPs, if mass transfer is to be sustained, heat must be continuously supplied to the higher pressure end and removed from the lower pressure end. A temperature driving force is needed to facilitate this transfer. The heat and mass transfer are in series, one after the other. Thus ChHP's batch cycle is either mass transfer limited or heat transfer limited. The evaporation/condensation of the working fluid is the basis of storage of heat in ChHPs. Therefore, the latent heat of vaporization of the working fluid will play an important role in deciding the energy densities of a ChHPs.

A literature review was performed to obtain chemical properties of the reactants utilized in the calcium oxide hydration/dehydration reaction. Three literature sources with applicable property data were obtained (Samms and Evans 1968; Schaube 2011; Schaube et al. 2012). The calcium oxide hydration/dehydration reaction equilibrium temperature versus pressure data from each of these sources was reproduced in Figure 7, which projects these data onto a benchmark plot of equilibrium readings to verify the mathematical expressions used in the calculations. The equilibrium data mathematical relationships utilized in this work are plotted as a color overlay to the original plot from Schaube et al. (2012), which is reproduced in black lines and symbols.

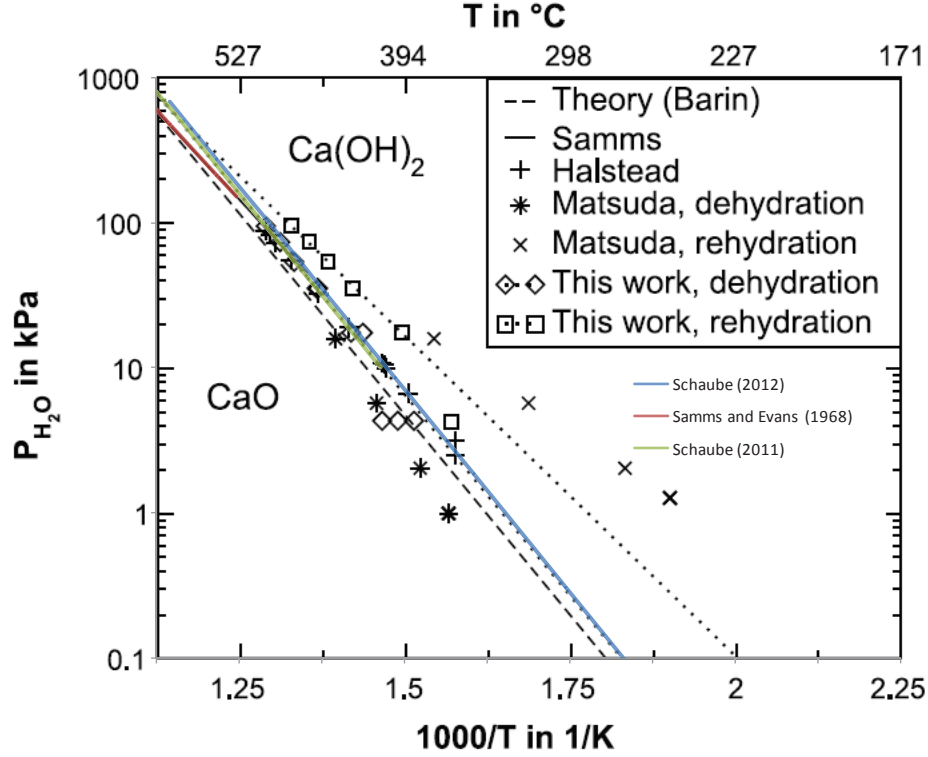


Figure 7. Equilibrium of  $\text{Ca(OH)}_2 \leftrightarrow \text{CaO} + \text{H}_2\text{O}$ .

The expression for the calcium oxide dehydration reaction temperature-pressure dependence was reported as:

$$\ln\left(\frac{P_{eq}}{10^5}\right) = -\frac{-12845}{T_{eq}} + 16.508$$

Where

$P_{eq}$  = equilibrium pressure in kPa

$T_{eq}$  = equilibrium temperature in K.

In order for the data in Figure 7 to be successfully reproduced, this equation had to be corrected to the following expression:

$$P_{eq} = 16.508 \times 10^8 \cdot \exp\left(\frac{-12845}{T_{eq}}\right)$$

Consequently, this corrected form of the equilibrium relationship was used in place of the reported expression for all relevant calculations.

From 7 it can be seen that there is good agreement between the relationships reproduced by this study with the values reported in the literature. The dehydration data from Schaub et al. (2012) is in good agreement with other literature data, and was therefore used as the primary source of calcium oxide hydration/dehydration equilibrium in this study.

A Clausius-Clapeyron diagram was constructed to illustrate the high and low-temperature reactor operating lines for a temperature amplification chemical heat pump process based on the hydration/dehydration of calcium oxide. This diagram is presented in Figure 8. Data from Samms and Evans (1968) and Schaub et al. (2012) were used to represent the equilibrium relationship between

calcium oxide and calcium hydroxide, which corresponds to the high-temperature reactor in this ChHP system. The low-temperature reactor operating line corresponds to the equilibrium relationship between water and steam. Saturated steam temperature versus pressure data from Sonntag (1986) and Lemmon et al. (2010) were found to be in very good agreement. The Sonntag water-steam equilibrium data was utilized in this study as the data exists in the form of a numerical correlation that facilitated subsequent analyses.

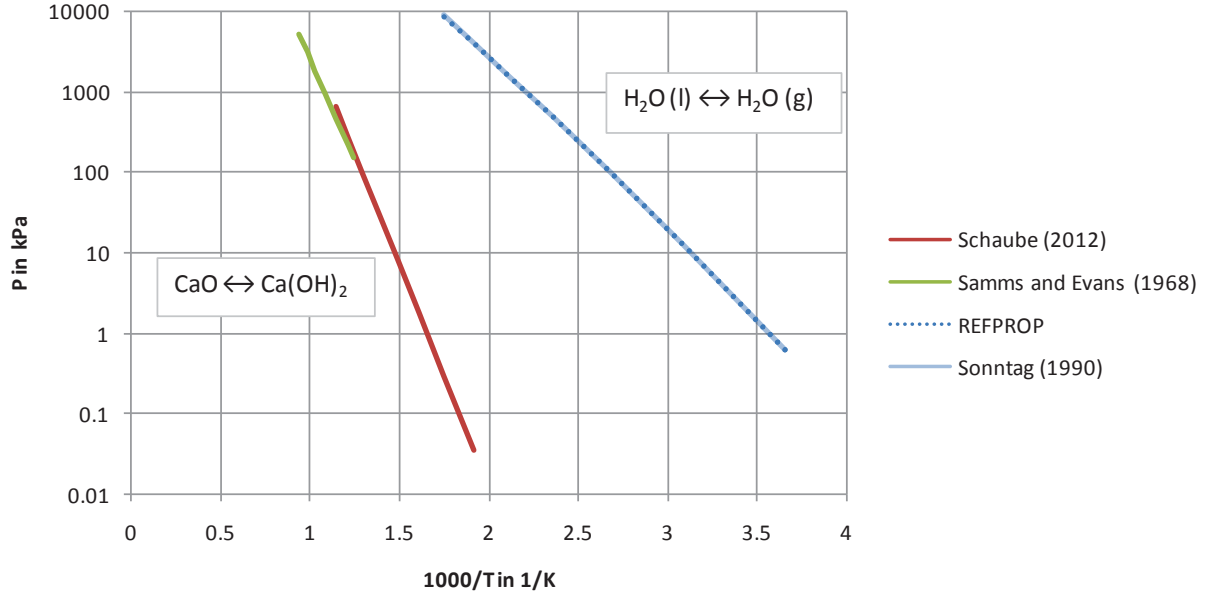


Figure 8. Clausius-Clapeyron diagram for the hydration/dehydration of calcium oxide.

The calcium oxide hydration/dehydration chemical heat pump is a potential candidate for upgrading LWR outlet temperature. In this system, the LWR reactor would provide heat at the medium temperature level,  $T_M$ , for generating steam for the calcium oxide hydration process (synthesis) as well as driving the calcium hydroxide dehydration process (regeneration). The high-temperature reactor would release heat at an elevated temperature  $T_H$  during the synthesis operation phase while the low-temperature reactor would reject heat from the cycle at a low-temperature  $T_L$  during the regeneration operation phase.

## 5.1 Process Conditions

In the temperature amplification ChHP, selection of the chemical working pair, the medium temperature level, and the system pressure losses determines the process conditions of the high and low temperature reactors (Raldow 1981). In this preliminary analysis, system pressure losses were neglected to simplify the analysis. The LWR outlet temperature was assumed to be 300°C. A Clausius-Clapeyron diagram including the high and low-temperature reactor operating lines and the process conditions corresponding to the operation of a calcium oxide hydration/dehydration temperature amplification ChHP process with heat input at  $T_M = 300^\circ\text{C}$  is illustrated in Figure 9. As shown in Figure 9, the 300°C heat input temperature results in high-temperature output and heat rejection temperatures of 787 and  $-9^\circ\text{C}$ , respectively. The pressures of the synthesis and regeneration operating steps are 9053 and 0.3 kPa, respectively.

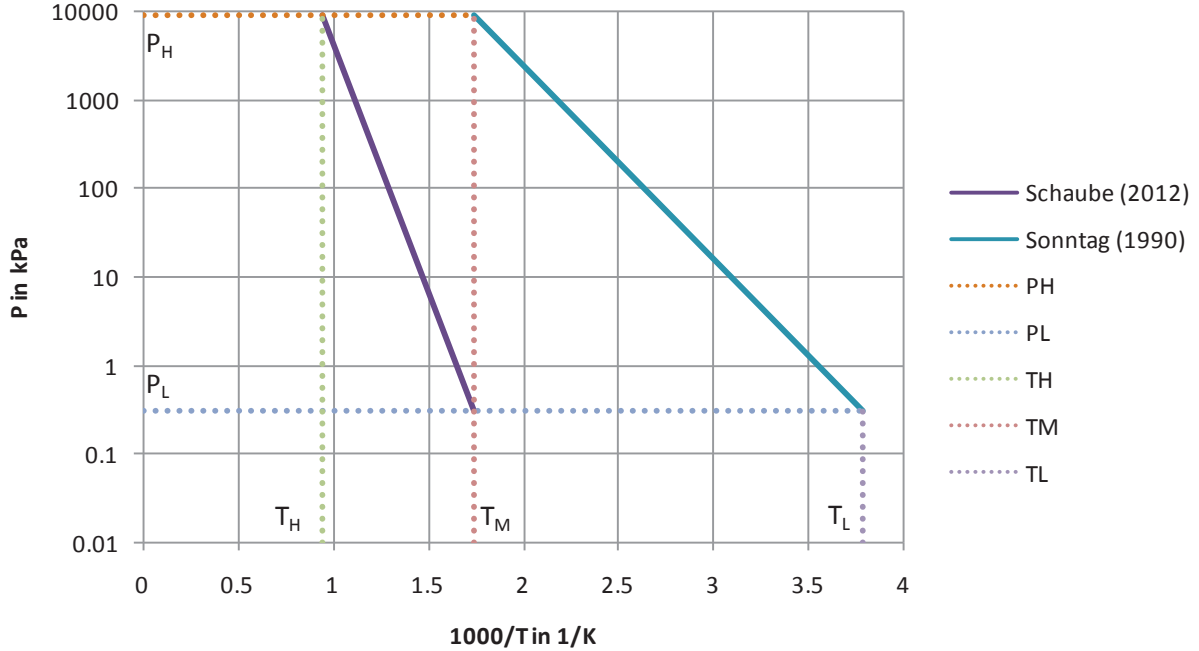


Figure 9. Calcium oxide hydration/dehydration temperature amplification ChHP for upgrading LWR outlet temperature

The heat rejection temperature of  $-9^{\circ}\text{C}$  is well below typical ambient temperature conditions, which is indicative that operation of a temperature upgrading ChHP, as described above, would not be feasible. In order for such a ChHP to be realized, one of several modifications would be required:

- Increase the heat input temperature  $T_M$  (impractical for LWR application)
- Implementation of a sub-ambient temperature heat rejection process that could utilize a refrigeration process (possibly an absorption or ChHP-based refrigeration process)
- Selection of a different chemical working pair (or a multistage ChHP temperature upgrade process).

The multistage ChHP temperature upgrade process described in the final bullet would require the LWR temperature upgrade process to occur in at least two stages: a working pair with an intermediate temperature output level could be used to provide heat input to the calcium oxide hydration/dehydration ChHP at a temperature above  $300^{\circ}\text{C}$ . Although not investigated as part of this study, magnesium oxide hydration/dehydration is a working pair that may be suited for this application.

## 5.2 Efficiency Calculations

Thermal efficiencies of the theoretical calcium oxide hydration/dehydration ChHP for LWR temperature upgrading applications are described in the following sections. The efficiency is estimated using two calculations: the first based on enthalpy of reaction, and the second based on operating temperature levels.

### 5.2.1 Enthalpy of reaction

The thermal efficiency of a temperature upgrading ChHP (chemical heat transformer) may be estimated from the heat of reaction of the high and low-temperature reactors. Useful heat  $\Delta H$  is released at  $T_H$  during the high-temperature exothermic reaction while heat input  $\Delta H_e$  occurs at  $T_M$  in the steam evaporator. In this case, the efficiency is given by the formula (Aristov 2008):

$$\eta_{thermal} = \frac{\Delta H}{(\Delta H_e + \Delta H)} < 1$$

Temperature upgrade via ChHP is a batch process, with changes to reactor conditions required to alternate between synthesis and regeneration operating stages. The above expression does not include any terms to account for these changes in the sensible heat of the reactants (or the associated process equipment). Raldow (1981) states that sensible heat terms are generally neglected and that standard values of reaction enthalpies are used when estimating the thermal efficiencies of chemical heat pumps. This approach is corroborated and substantiated by Aristov (2008).

The calculation of all efficiencies is based on the common assumption that the expenditures of heat needed to change the heat capacity of the system are equal to zero, implying that the thermal mass of the system is ignored or a complete heat recovery in it is assumed. Even if the heat recovery is incomplete or is not possible at all, the expenditures for the heating of the system is usually small as compared to the heat of chemical reactions, which justifies the use of the above assumption for this case as well.

The thermal efficiency of the calcium oxide hydration/dehydration ChHP was estimated using the approach described above. The calcium oxide-based temperature amplification ChHP absorbs heat at temperature  $T_M$  under equilibrium conditions and the useful heat  $\Delta H$  is released during the exothermic calcium oxide hydration reaction at high-temperature  $T_H$ . Heat input  $\Delta H_e$  for vaporization of the steam in the low-temperature reactor (evaporator) would be provided by the LWR. Table 1 summarizes thermal efficiency estimates for upgrading LWR outlet temperature using a calcium oxide hydration/dehydration ChHP with process conditions corresponding to those described in the previous section. The various estimates provided in Table 1 correspond to different values of the calcium oxide hydration/dehydration reaction as provided by the literature sources specified.

Table 1. Thermal efficiency of calcium oxide hydration/dehydration ChHP using heat of reaction values reported in various literature sources.

$\text{CaO} + \text{H}_2\text{O} \leftrightarrow \text{Ca(OH)}_2$ $\Delta H$ (kJ/mol)	$\text{H}_2\text{O(l)} \leftrightarrow \text{H}_2\text{O(g)}$ $\Delta H$ (kJ/mol)	$\eta$ (%)
94.6 (Samms and Evans 1968)	43.9 (Lemmon et al. 2010)	68.3
104.3 (Halsted and Moore 1957)	43.9 (Lemmon et al. 2010)	70.4
106.8 (Schaube et al. 2012)	43.9 (Lemmon et al. 2010)	70.9

### 5.2.2 Temperature Level

The maximal theoretical efficiency of a temperature-amplification ChHP may also be estimated from the operating temperatures of the condenser, evaporator, and generator (high temperature reactor) (Aristov 2008):

$$\eta_{max} = \frac{(1/T_e - 1/T_c)}{(1/T_e - 1/T_g)}$$

Where:

$c$  = condenser

$e$  = evaporator



$g$  = generator (high temperature reactor).

This expression can alternatively be written as (Arjmand et al. 2012):

$$\eta_{\max} = \frac{T_H (T_M - T_L)}{T_M (T_H - T_L)}$$

Where:

$H$  = high

$M$  = medium

$L$  = low.

The maximal theoretical efficiency of the calcium oxide hydration/dehydration ChHP was calculated using a heat input temperature of  $T_M = 573$  K (300°C), with the corresponding heat output and heat rejection temperatures of  $T_H = 1060$  K (787°C) and  $T_L = 264$  K (-9°C) determined previously. The maximal theoretical efficiency corresponding to these temperatures is  $\eta_{\max} = 71.8\%$ . The thermal efficiency values calculated in the previous section are below this theoretical upper bound.

## 6. ENVIRONMENTAL LIFE CYCLE ASSESSMENT

The use of ChHPs will result in avoiding of greenhouse gas emissions of equivalent fossil fuel usage. However, the true environmental cost of the process and net benefits can only be determined through the Life Cycle Assessment (LCA), which is a useful tool for quantification of the environmental impacts of any activity, process, or product. LCA of the ChHP-biomass system shown in Figure 5 was initiated to understand its environmental impact, which can then be used for comparison with various alternative technologies for the synthesis of transportation fuels. LCA involves the following four steps: *Goal Definition and Scoping* (defining system boundaries), *Inventory Analysis* (identifying and quantifying the consumption and release of materials), *Impact Assessment* (assessing the effects of these activities), and *Interpretation* (evaluation of the results). The system boundary will be defined to include the nuclear reactor as well as the fuel synthesis process.

The first step in the LCA process is the selection of the biomass to be used in the synthesis process. The biomass to be used in the process must have the desirable characteristics of sustainability, short life cycle (so that it is repeatable and reproduces fast), geographically non-specific, and should not require intense industrial input for harvesting. Several biomass materials were considered for advanced study, such as industrial and municipal waste products, food-crops, water-based organics such as algae, and cellulosic biomass. The source selected was cellulosic for two reasons: it does not impact the food supply and it is a consistent, predictable, and reliable reproducible product. Four cellulosic products are in consideration for the source material for this study: (1) food-crop wastes, (2) brush materials, such as reeds, willows, and sage, (3) grasses, such as prairie grasses and switch grass, and (4) trees, such as poplar and pine. Depending on the geographic location where the biomass plant would be located, these four products prove to be more or less beneficial. This study focuses on trees as the source of biomass.

Forests, trees particularly, are the largest storers of CO<sub>2</sub> on the planet. When forest debris naturally aerobically biodegrade, they produce measurable amounts of Acetylene and Phenols (Schniewind 1989). When they degrade anaerobically through a process called pyrolytic gasification, they produce these same chemicals—methane, carbon dioxide, and a resultant product called bio-char. All of these products have defined transfer paths to become synthetic fuels, except bio-char, which is an excellent bio-rejuvenator (IBI 2013).

The three potential alternatives examined included poplar (*Populus*), pine (*Pinus*), and corn. Corn has received attention due to its potential for conversion to ethanol; however, is eliminated from consideration here due to its value as a food crop. Pine and poplar are softwoods and grow rapidly; they are also hardy, adaptable to most U.S. environments, grow naturally, and require little maintenance. Pine, due to the



nature of the current genetic modification science, does not grow in a limbless or easily accessed (by equipment) varieties. Poplar trees have been the focus of several scientific studies and grow in several modified formats (Marchadier and Sigaud 2005). Poplars are also able to be grown in closer proximity and produce larger yields per acre-year of chipped material. Essentially, poplar can be grown and harvested cyclically in a small space with high and sustainable yields. Poplar is an attractive alternative, due to its potential for carbon-neutrality, low-energy requirements, and fast growth. Canadian University of Guelph has performed extensive renewable energies research specific to woody biomass materials. One of the in-depth research areas is their growth farm. Two the products grown there are willow and poplar, which act as symbiotic growth enhancers, with poplar supporting an aggressive growth cycle allowing for a 3-year plant-harvest cycle that can be repeated up to seven times before another more rejuvenating product to be planted. Willow is the sister product of poplar in the mentioned study, supporting an active growth cycle that rejuvenates the earth in preparation for the poplar cycles to begin again.

Genetically modified poplar is proposed to be used as the base biomass material, with minor willow constituents during off-peak cycles.

## **7. FUTURE WORK AND PATH FORWARD**

The project supported two doctoral level graduate students: the screening and thermodynamic analysis of ChHPs was being conducted by Daniel Wendt, a Ph.D. student in chemical engineering, while the systems analysis/life cycle study was being conducted by Jeffrey Heath.

The future steps for advancing the NHES utilizing ChHP technology include:

1. Detailed thermodynamic analysis of the ChHP.
2. Initiation of bench-scale experimentation on the ChHP, to demonstrate the proof-of-concept and scale-up to demonstrate the feasibility.
3. Conceptual design of the LWR-ChHP-Biomass Processing system, and techno-economic analysis.
4. Comprehensive LCA of the system.

## 8. REFERENCES

- Abel, C. R., *Patent No. US 2012/0039439*. USA, 2012.
- Angelino, G. and Invernizzi, C. (1995). Prospects for real-gas reversed Brayton cycle heat pumps. *Int. J. Refrig.* 18 (4) 272-280.
- Aristov, Y. I., "Chemical and Adsorption Heat Pumps: Cycle Efficiency and Boundary Temperatures," *Theoretical Foundations of Chemical Engineering*, 42(6), 873–881, 2008.
- Arjmand, M., L. Liu, and I. Neretnieks, "Exergetic efficiency of high-temperature-lift chemical heat pump (ChHP) based on  $\text{CaO}/\text{CO}_2$  and  $\text{CaO}/\text{H}_2\text{O}$  working pairs," *International Journal of Energy Research*, 2012.
- Azpiazu, M. N., J. M. Morquillas, and A. Vazquez, "Heat recovery from a thermal energy storage based on the  $\text{Ca}(\text{OH})_2/\text{CaO}$  cycle," *Applied Thermal Engineering*, 23, 733–741, 2003.
- Cot-Gores, J., A. Castell, and L. F. Cabeza, "Thermochemical Energy Storage and Conversion: A-State-of-the-Art Review of the Experimental Research Under Practical Conditions," *Renewable and Sustainable Energy Reviews*, 16, 5207–5224, 2012.
- Fujimoto, S., E. Bilgen, and H. Ogura, " $\text{CaO}/\text{Ca}(\text{OH})_2$  chemical heat pump system," *Energy Conversion and Management*, 43, 947–960, 2002.
- Fujimoto, S., E. Bilgen, and H. Ogura, "Dynamic simulation of  $\text{CaO}/\text{Ca}(\text{OH})_2$  chemical heat pump systems," *Exergy*, 2, 6–14, 2002.
- Guo, J., and X. Huai, "Optimization design of recuperator in a chemical heat pump system based on entransy dissipation theory," *Energy*, 41, 335–343, 2012.
- Halstead, P. E. and A. E. Moore, "The thermal dissociation of calcium hydroxide," *Journal of the Chemical Society*, 3873–3875, 1957.
- Hasatani, M., "Highly Developed Energy Utilization by use of Chemical Heat Pump," In *Global Environment Protection Study Through Thermal Engineering*, 1992, pp. 313–322.
- Heat Pump Centre. (2007). Heat Pumps in Industry. Retrieved May 9, 2013, from Heat Pump Centre: <http://www.heatpumpcentre.org/en/aboutheatpumps/heatpumpsinindustry/Sidor/default.aspx>
- Kato, Y., K. Kobayashi, and Y. Yoshizawa, "Durability to Repetitive Reaction of Magnesium Oxide/Water Reaction System for a Heat Pump," *Applied Thermal Engineering*, 18(3-4), 85–92, 1998.
- Kato, Y., Y. Sasaki, and Y. Yoshizawa, "Magnesium oxide/water chemical heat pump to enhance energy utilization of a cogeneration system," *Energy*, 30, 2144–2155, 2005.
- Kato, Y., F. Takahashi, A. Watanabe, and Y. Yoshizawa, "Thermal Performance of a Packed Bed Reactor of a Chemical Heat Pump for Cogeneration," *Chemical Engineering Research and Design*, 78(5), 745–748, 2000.
- Kato, Y., F.-u., Takahashi, A. Watanabe, and Y. Yoshizawa, "Thermal analysis of a magnesium oxide/water chemical heat pump for cogeneration. *Applied Thermal Engineering*, 21, 1067–1081, 2001.
- Kato, Y., N. Yamashita, K. Kobayashi, and Y. Yoshizawa, "Kinetic Study of the Hydration of Magnesium Oxide for a Chemical Heat Pump," *Applied Thermal Engineering*, 16(11), 853–862, 1996.
- KlinSoda, I. and P. Piumsomboon, "Isopropanol-acetone-hydrogen chemical heat pump: a demonstration unit," *Energy Convers. Mgmt.*, 48, 1200–1207, 2007.

- Kyaw, K., T. Shibata, F. Watanabe, H. Matsuda, and M. Hasatani, "Applicability of Zeolite for CO<sub>2</sub> Storage in a CaO-CO<sub>2</sub> High Temperature Energy Storage System," *Energy Convers Mgmt.*, 38(10-13), 1025–1033, 1997.
- Le Goff, P., H. Le Goff, A. Soetrisnanto, and J. Labidi, "New techniques for upgrading industrial waste heat," *Experimental Thermal and Fluid Science*, 7(2), 132, 1993.
- Lemmon, E., M. Huber, and M. McLinden, "NIST Standard Reference Database 23: Reference Fluid Thermodynamic and Transport Properties-REFPROP," Version 9.0. Gaithersburg, MD: National Institute of Standards and Technology, Standard Reference Data Program, 2010.
- Mills, J. I. and R. N. Chappell, "Advanced Mechanical Heat Pump Technologies for Industrial Applications," *Proceedings from the Seventh National Industrial Energy Technology Conference, Houston, Texas, 1985*, pp. 471–478.
- Ogura, H., H. Ishida, H., R. Yokooji, H. Kage, Y. Matsuno, and A. S. Mujumdar, "Experimental Studies on a Novel Chemical Heat Pump Dryer using a Gas-Solid Reaction," *Drying Technology*, 19(7), 1461–1477, 2001.
- Ogura, H., R. Shimojyo, H. Kage, Y. Matsuno, and A. S. Mujumdar, "Simulation of Hydration/Dehydration of CaO/Ca(OH)<sub>2</sub> Chemical Heat Pump Reactor for Cold/Hot Heat Generation," *Drying Technology*, 17 (7&8), 1579–1592, 1999.
- Ogura, H., T. Yamamoto, H. Kage, Y. Matsuno, and A. S. Mujumdar, "Effects of heat exchange condition on hot air production by a chemical heat pump dryer using CaO/H<sub>2</sub>O/Ca(OH)<sub>2</sub> reaction," *Chemical Engineering Journal*, 86, 3–10, 2002.
- Ogura, H., S. Yasuda, Y. Otsubo, and A. Mujumdar, "Continuous operation of a chemical heat pump," *Asia-Pacific J. Chem. Eng.*, 2, 118–123, 2007.
- Olszewski, M., and A. Saltash, "High-lift chemical heat pump technologies for industrial processes," *1995 ASME International Congress and Exposition, 1995*.
- Park, C., M. Patterson, V. Maio, and P. Sabharwall, "Dependable Hydrogen and Industrial Heat Generation from the Next Generation Nuclear Plant," *Proceedings of National Hydrogen Association*. Columbia, South Carolina, 2009.
- Raldow, W., "Thermal efficiencies of chemical heat pump configurations," *Solar Energy*, 27, 307–311, 1981.
- Samms, J. A. and B. E. Evans, "Thermal Dissociation of Ca(OH)<sub>2</sub> at Elevated Pressures," *J. Appl. Chem.*, 18, 5–8, 1968.
- Schaube, F., "High Temperature Thermochemical Heat Storage for Concentrated Solar Power Using Gas-Solid Reactions," *Journal of Solar Energy Engineering*, 133, 031006-1 - 031006-7, 2011.
- Schaube, F., L. Koch, A. Worner, and H. Muller-Steinhagen, "A thermodynamic and kinetic study of the de- and rehydration of Ca(OH)<sub>2</sub> at high H<sub>2</sub>O partial pressures for thermochemical heat storage," *Thermochim. Acta*, 538, 9–20, 2012.
- Schaube, F., A. Worner, and H. Muller-Steinhagen, "High Temperature Heat Storage Using Gas-Solid Reactions," *11<sup>th</sup> International Conference on Energy Storage*, Stockholm, Sweden, 2009.
- Sonntag, D. (n.d.), "Important new values of the physical constants of 1986, vapour pressure formulations based on the ITS-90, and psychrometer formulae," *Z. Meteorol.*, 40, 340–344.
- Thermea Energiesysteme. (2008) High Temperature Large Scale Heat Pumps for Industrial Use. Retrieved May 9, 2013, from Everything R744: [http://www.r744.com/assets/link/thermea\\_broschuere\\_short.pdf](http://www.r744.com/assets/link/thermea_broschuere_short.pdf)

Wongsuwan, W., S. Kumar, S., P. Neveu, and F. Meunier, “A Review of Chemical Heat Pump Technology and Applications,” *Applied Thermal Engineering*, 21, 1489–1519, 2001.

# Appendix A

## Literature Review of Inorganic Chemical Heat Pump Research

### CaO/Ca(OH)<sub>2</sub> Chemical Heat Pumps

Hasatani (1992) performed CaO hydration/dehydration chemical heat transformer proof of concept experiments. To generate steam at 640 K, as would be required to release heat at a temperature of 1205 K in the high-temperature CaO reactor, a system pressure of 27.5 MPa would be required as indicated in Figure A-1. During heat release experiments, the evaporator was operated at a pressures up to 0.142 MPa (430 K saturated steam). The CaO bed generated heat at a temperature of 800 K at the maximum evaporator pressure of 0.142 MPa. Temperatures at various axial positions in the cylindrical CaO reactor were recorded as a function of reaction time. The proof of concept experiments verified that the pseudo-equilibrium temperature of the CaO hydration reaction shifted to higher temperatures with increasing steam pressures. Following completion of the CaO hydration reaction, large radial temperature gradients in the reactor bed were observed, suggesting that the heat transfer characteristics of the reactor bed were insufficient. Passive heat transfer augmentation techniques were implemented to enhance the heat transfer rate. Condenser performance was deemed insufficient to condense the large quantity of superheated steam released from the reactor at the start of the dehydration reaction, and development of a high-performance evaporator/condenser was recommended as an important requirement for realization of the CaO hydration/dehydration ChHPs.

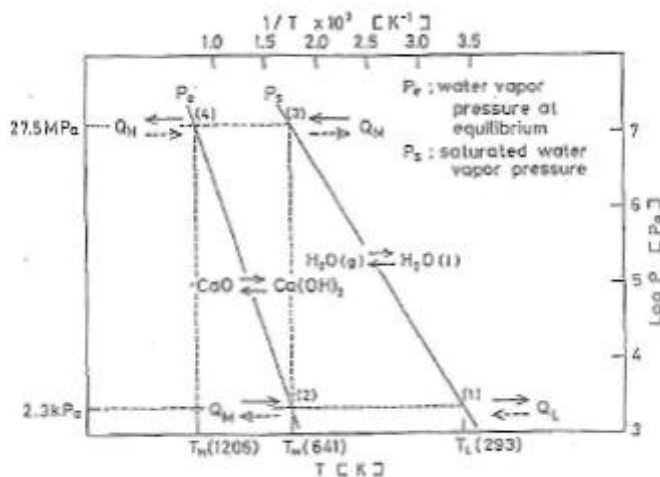


Figure A-1. Temperature-pressure line (Hasatani 1992).

Fujimoto et al. (2002a) formulated a theoretical model to simulate dynamic behavior of a CaO hydration/dehydration reactor coupled with an evaporator condenser. The model was validated against experimental results. The simulation was deemed to adequately model chemical heat pump performance of the system for heating and cooling applications. The heat pump studied utilized heat input at 673 K for dehydration with condensation occurring at 293 K. The water was vaporized at 290 K and the heat of hydration was utilized to supply heat at a temperature of 353 K. The Clausius-Clapeyron diagram is included as Figure A-2. The model included mass and energy conservation equations for the CaO hydration/dehydration reactor and condenser/evaporator with inclusion of terms for heat transfer associated with resistance heater input, evaporator heating load, and condenser cooling load; and reactor bed heat loss, hydration/dehydration reactor heat of reaction, and mobile phase energy flow. State equations for reactor and evaporator/condenser pressure-temperature equilibrium relations are included as

well as kinetic rate equations for CaO hydration and dehydration from Matsuda et al. (1985). Simplifying assumptions included perfectly mixed cooling water in cooling coils, uniform dehydration temperature throughout the particle bed, and that the reactor and particle mass remained at equal temperatures  $T_M \cong T_P$  throughout the dehydration/hydration operations.

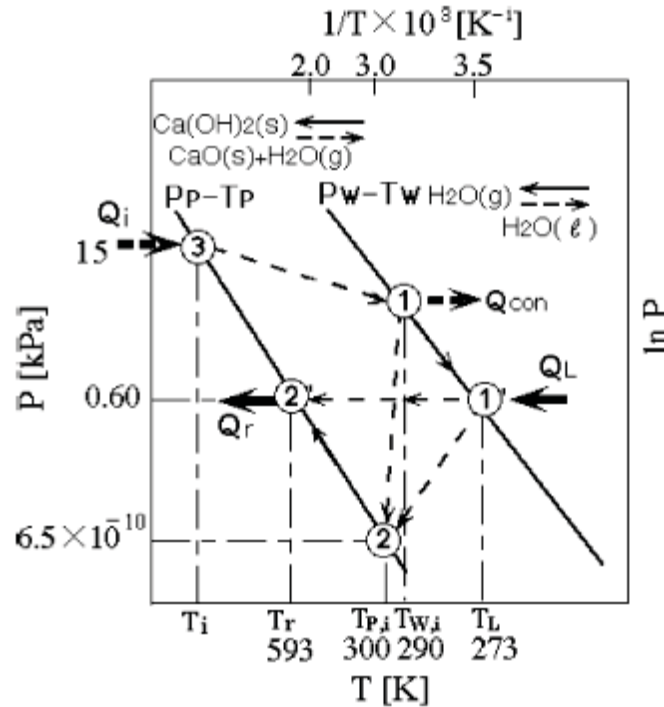


Figure A-2. Thermodynamic diagram of CaO/Ca(OH)<sub>2</sub> chemical heat pump system (Fujimoto, Bilgen, and Ogura, CaO/Ca(OH)<sub>2</sub> chemical heat pump system, 2002).

Fujimoto et al. (2002b) utilizes the dynamic model described in Fujimoto et al. (2002a) to simulate a CaO hydration/dehydration reaction system for residential dwelling heating and cooling applications. The additional assumption is included such that during the dehydration step hydration never occurs and, similarly, during the hydration step dehydration never occurs. System sizing calculations were performed and results of a simulation where the heating and cooling demands vary as a function of time were presented. The authors concluded that a CaO/Ca(OH)<sub>2</sub> chemical heat pump system could satisfactorily respond to heating and cooling demands of a typical dwelling. Thermal and exergy efficiencies of 58.7% and 61.6% for heating applications and 12.7% and 4.5% for cooling applications, respectively, were reported.

Ogura et al. (1999) developed a two dimensional reactor model to simulate the heat and mass transfer behavior of a CaO/Ca(OH)<sub>2</sub> chemical heat pump. Simulation theoretical results were compared against heat release step experimental results in which water was evaporated at a temperature of 290 K to provide steam to the exothermic CaO hydration reactions for heat production at a temperature of approximately 627 K, as shown in Figure A-3. The theoretical model simulated heat and mass transfer in the radial and axial dimensions with equilibrium pressure based on the data of Halstead and Moore (1957) and the CaO reaction rate based on kinetic data from Matsuda et al. (1985). Effective thermal conductivity, specific heat, and density were allowed to vary over the course of the simulation while the thermal contact resistances between the particle bed and cooling pipe as well as between the particle bed and reactor wall were kept constant throughout the simulation. Steam macro-flow through the particle bed was modeled using the Kozeny-Carman equation and steam micro-flow was determined using a diffusion coefficient calculated by the Slattery-Bird equation. Reaction rates, temperature distributions, pressure distributions,

etc., as a function of time are simulated using a finite difference method. Three model formulations were developed in which steam mass flow and mass diffusion were alternately considered and disregarded. Model results indicate that the mass transfer resistance of the reactor bed results in a pressure distribution within the bed and that the steam cannot move inside the reactant bed fast enough to hydrate the CaO due to the mass transfer resistance in the bed and the stagnant zone outside the bed.

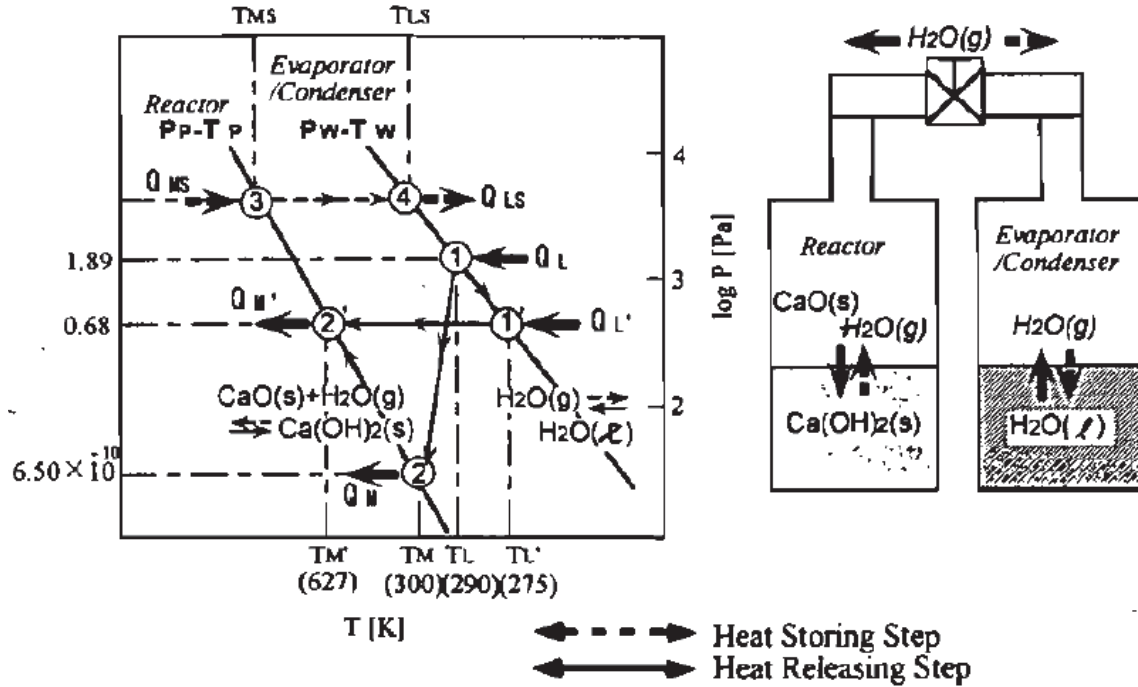
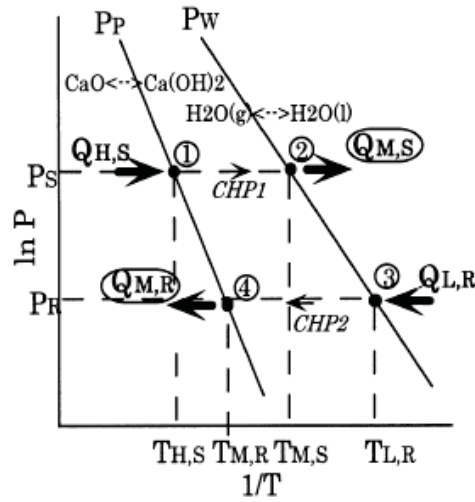


Figure A-3. Schematic diagram of the operation principle.

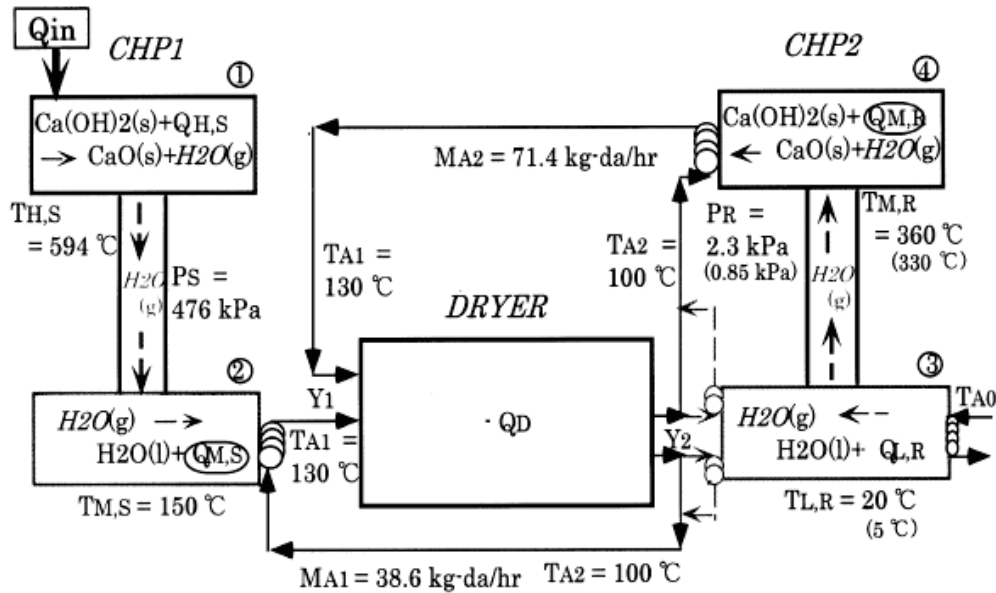
Ogura et al. (2001) performed a basic, exploratory experimental study to test the effectiveness of a chemical heat pump based on the  $CaO/H_2O/Ca(OH)_2$  gas-solid reversible hydration/dehydration reaction for drying applications. The ChHP was operated in heat enhancement, or heat amplification, mode since this mode has the highest energy efficiency, releasing useful heat even in the heat-storing step. The heat produced by the ChHPs was transferred to air or water heat transfer fluids via heat exchanger where it could be directly (air) or indirectly (water) used to provide a heat source for convective drying, as shown in Figure A4. The refrigeration duty produced by the ChHPs could potentially be used to provide dehumidification of the dryer air. The ChHP dryer requires two  $CaO/Ca(OH)_2$  hydration/dehydration reactor units as indicated in Figure A4. Each unit consisted of a CaO reactor bed, an evaporator/condenser, as well as the required heat exchange equipment, heating/cooling coils, instrumentation, etc. Each unit operated alternatively in heat storage and heat release mode. High temperature heat was stored in the CaO reactor at a temperature of 594°C or greater. The condenser released medium temperature heat around 150°C. When operating in heat-release mode, the ChHP release medium temperature heat around 360°C generated from CaO hydration reactions with steam produced in the evaporator at around 20°C. In summary, the ChHP system stored the 600°C heat and released 150 and 360°C heat continuously by switching the operation of each of the two ChHPs units. Air and water were both tested as heat exchange medium in the experiments, although the specific apparatus used in these experiments was originally designed for hot water production and proved not to be an ideal configuration for hot air production. In addition to varying the heat exchange medium, experiments included varying mass of CaO particles in the reactor and the evaporator water temperature. The final CaO conversion of the hot air heat exchange experiments exceeded that of the hot water heat exchange experiments, indicating that the air heat exchange did not adversely affect the ChHPs reaction. However, the generated



heat is not recovered effectively in the hot air heat exchange experiment, resulting in bed temperatures that remain at elevated temperature for longer than in the hot water heat exchange experiments. This was attributed to the low-heat transfer rate between the reactor wall and the air stream. The optimum required air flow rate was calculated and found to be significantly greater than the flow rate capability of the experimental unit. Heat recovery efficiencies were presented for various experimental conditions, and the proposed ChHP dryer was found to produce hot air at temperature levels and with reaction rates and conversions as good as in the case of hot water production. An experiment with a 6.0 kg CaO reactor bed generated higher temperature hot air than an experiment with a 4.8 kg CaO reactor bed. Heat recovery efficiencies ranged from 16.7% for the 6.0 kg CaO bed with 286 K evaporator water to 22.9% for the 4.8 kg CaO bed with 279 K evaporator water. Output power (heat rate) was found to increase with increasing reactant mass and increasing evaporator water temperature.



a) Operating line



b) Flowsheet

Figure A4. ChHPs system using CaO/H<sub>2</sub>O/Ca(OH)<sub>2</sub> reaction operating in heat enhancement.



The chemical heat pump dryer reactor design documented in Ogura et al. (2001) was modified for the experiments of Ogura et al. (2002) to include a “wide mesh heat exchanger” for accommodating larger air flow rates. The wide mesh heat exchanger included an acrylic cylinder with a stainless steel mesh packed between the reactor and the acrylic cylinder. A schematic of the modified experimental reactor is shown in Figure A-5. Experiments showed that the heat exchanger design and the air flow rate both have an effect on heat recovery efficiency. The heat recovery efficiency was increased to 37.4% using the wide mesh heat exchanger. Experiments were performed in which the air flow rate was increased by a factor of four, resulting in an increase in the heat recovery efficiency from 12.3% to 50.56%. The heat recovery efficiency increased by more than four times in conjunction with the air flow increase, indicating that the air flow rate was not sufficiently high to recover the reactor heat generated in the experiments. Investigation into the causes of low CaO conversion efficiency and low-heat recovery efficiency indicated that significant mass transfer resistance existed along the reactor vertical axis for water vapor diffusion. It was concluded that the reactant bed must be shallow in the water vapor flow direction to reduce the mass transfer resistance. Additionally, the reactor and heat exchanger design should incorporate methods for increasing the convective heat transfer coefficient because the heat recovered by the air heat exchanger is governed by that released from the reactor wall.

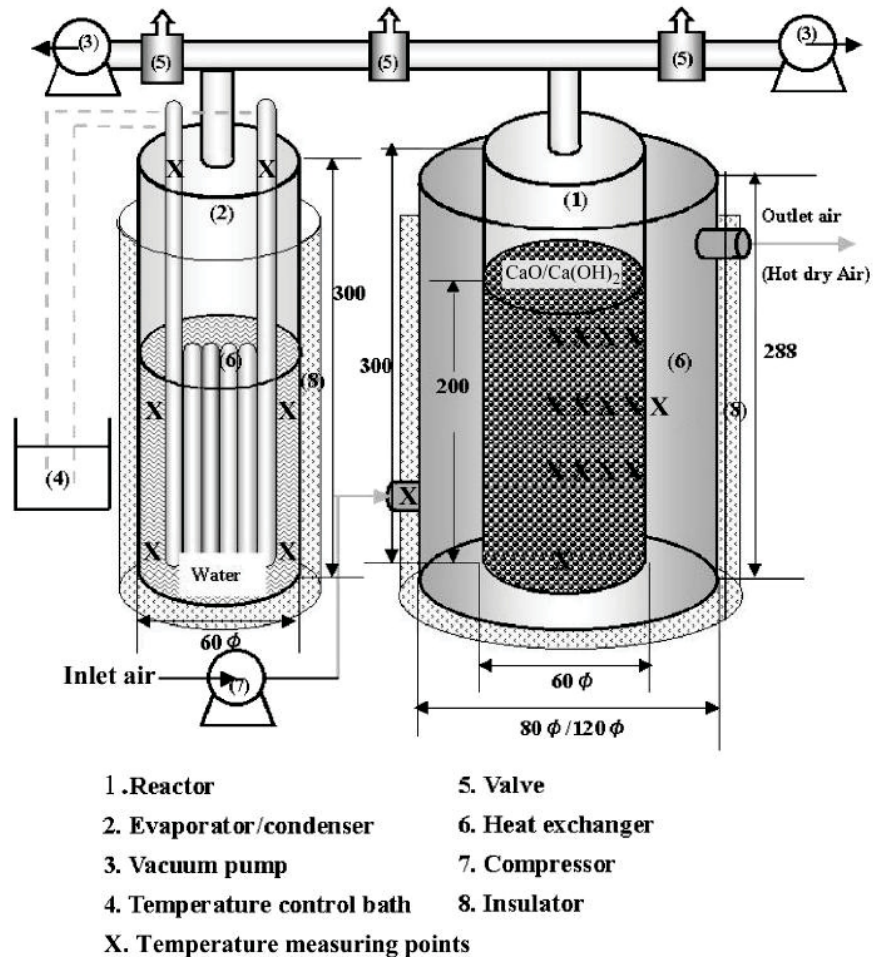


Figure A-5. Standard-type ChHPs unit (Ogura, Yamamoto, Kage, Matsuno, and Mujumdar 2002).

Schaube et al. (2009) compared CaO hydration-dehydration and carbonation-decarbonation reactions for elevated temperature storage applications. The CaO/Ca(OH)<sub>2</sub> and CaO/CaCO<sub>3</sub> systems (as shown in

Figure A-6) were chosen for their ability to store and release heat with operating pressures around 1 bar. The researchers investigated a fixed bed with use of a gas medium to transport the heat of reaction. Formulation of a mathematical model incorporating mass balances for the solid and gas phases, momentum balance for the gaseous phase, and energy balance for the gas and solid phases was discussed. The model was used to investigate effects of variation of kinetic parameters (pre-exponential factor) and the heat transfer coefficient. When the model reaction kinetics were decreased, the reaction provided less heat than the gas flowing through the reaction zone is capable of absorbing, resulting in cooling of the reaction zone with coinciding decreases in conversion rate and outlet gas temperature. A reduced heat transfer coefficient resulted in the gas not being able to take up as much heat, causing the reaction to take place at higher particle temperature. The reaction rate slowed down accordingly and the reaction zone expanded, producing a decreased reactor outlet temperature. The reaction was concluded to be restricted primarily by heat transport, with minor dependence on kinetics.

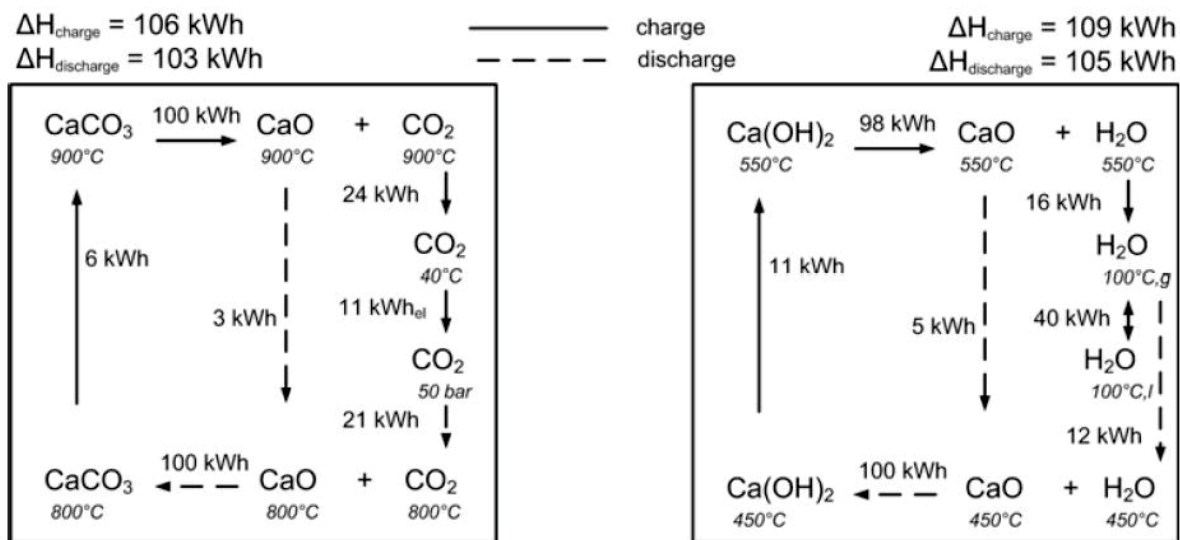


Figure A-6. Cycling characteristics, 1 bar CO<sub>2</sub>/H<sub>2</sub>O.

## CaO/CO<sub>2</sub> Chemical Heat Pumps

Kyaw et al. (1997) analyzed methods for storage of CO<sub>2</sub> generated during dissociation of CaCO<sub>3</sub> in a high temperature CaO-CO<sub>2</sub> thermal energy storage system. The authors considered three CO<sub>2</sub> storage systems: compressed gas, other metal carbonates, and adsorbents for CO<sub>2</sub> storage. The process flow diagram with a detailed inset of each CO<sub>2</sub> storage technology is shown in Figure A-7. The temperature-pressure behavior of each of the CO<sub>2</sub> storage systems is shown in Figure A-8. COPs for each system were evaluated and it was found that the system using zeolite for CO<sub>2</sub> storage was comparable with other systems and that its COP increased with increasing absorptivity Figure A-9.

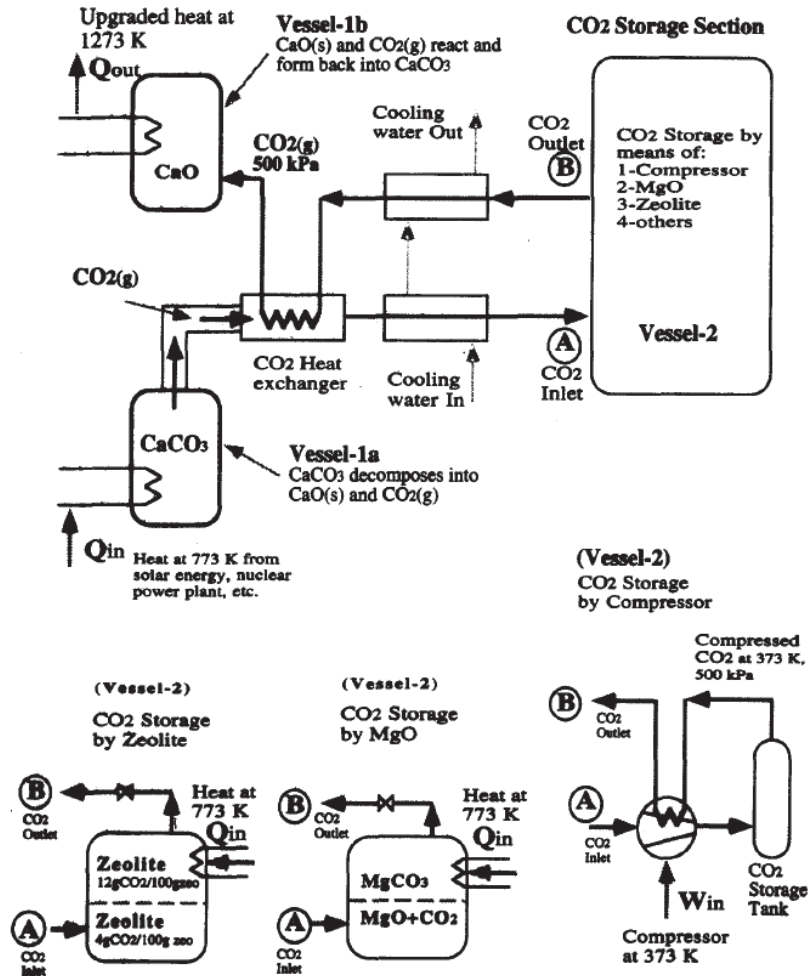


Figure A-7. Conceptual flow diagrams of CaO-CO<sub>2</sub> energy storage systems in a heat upgrading mode. Some CO<sub>2</sub> storage methods are shown in the bottom.

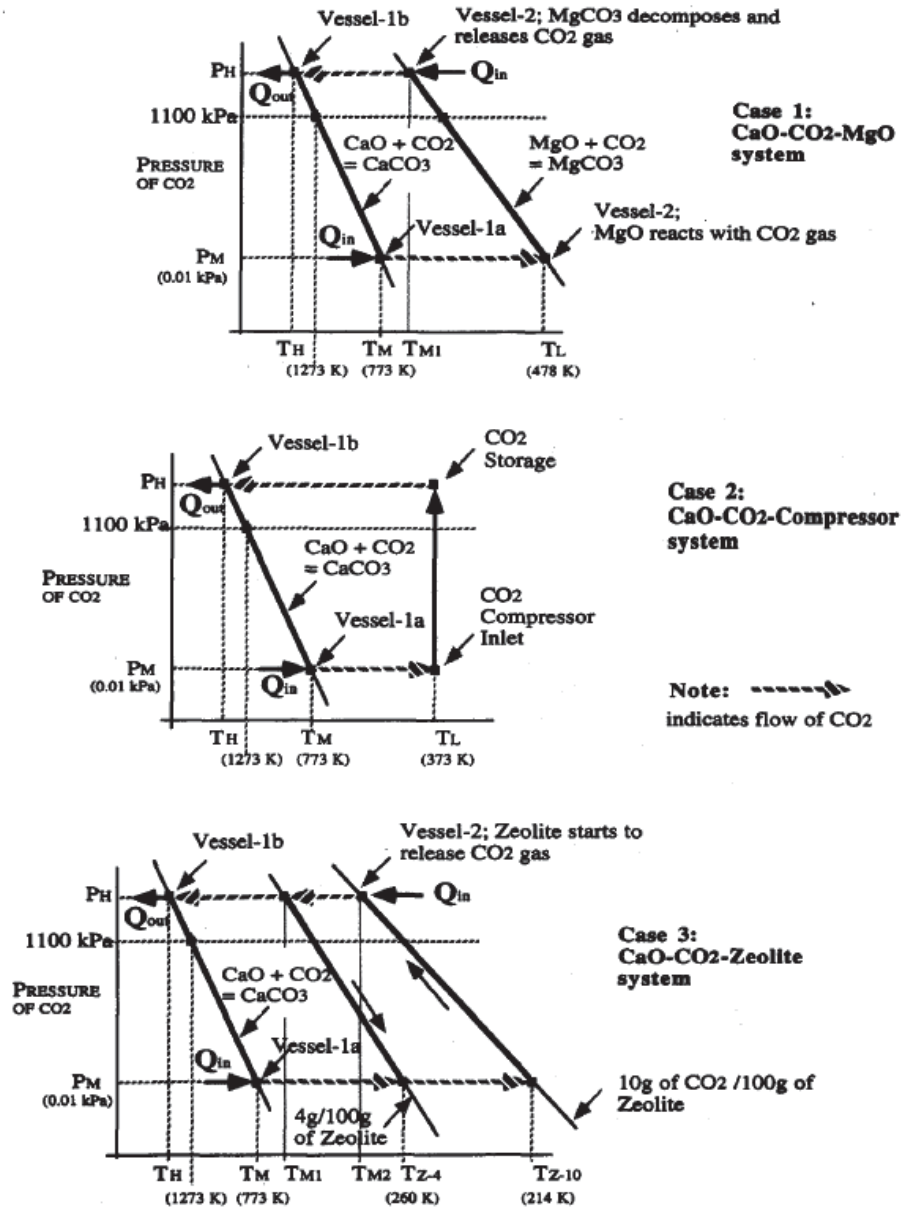


Figure A-8. Schematic diagrams of CaO-CO<sub>2</sub> energy storage systems with three different CO<sub>2</sub> gas storage methods.

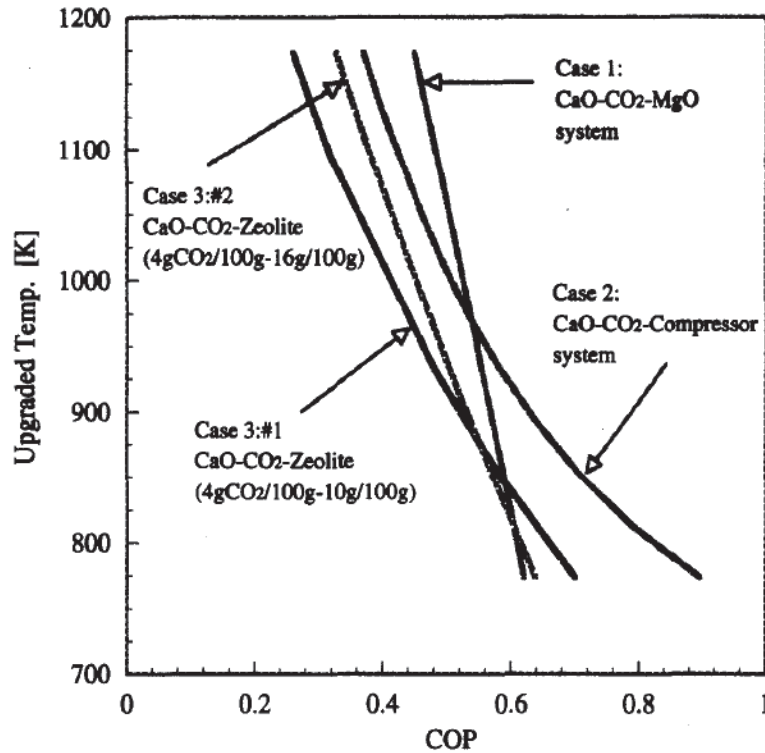


Figure A-9. COP vs. upgraded temperature of CaO-CO<sub>2</sub> energy storage systems with various CO<sub>2</sub> gas storage systems.

A thermal energy storage temperature amplifying system was proposed in which heat at 773 K was used for decomposing CaCO<sub>3</sub> at a pressure of 0.01 kPa. The CO<sub>2</sub> was adsorbed by zeolite at 214 K and 0.01 kPa. To initiate the temperature amplification, the zeolite was heated from 214 to 260 K, desorbing the zeolite from 10 to 4 g/100g and raising the CO<sub>2</sub> gas pressure from 0.01 to 1100 kPa. The desorbed CO<sub>2</sub> was preheated to 773 K (via heat exchange with an identical system that is operating in heat storage mode) before the gas was sent to react with CaO. At a pressure of 1100 kPa, the CO<sub>2</sub> and CaO produced the CaCO<sub>3</sub> product at an equilibrium temperature of 1273 K.

The authors performed experiments to determine the CO<sub>2</sub> adsorption equilibrium for zeolite 13X and super activated carbon. The volumetric method was used for adsorption experiments at temperatures from 287.5 to 573 K over a pressure range of 0 to 900 kPa. Both zeolite 13X and super-activated carbon adsorbed more gas at higher pressure and lower temperature. Neither adsorbent displayed significant tendency toward hysteresis. Adsorptivity of both adsorbents was most fittingly represented with Freundlich's expression,  $q = k \cdot P^{1/n}$ . Extrapolation of experimental results indicated that although zeolite 13X exhibited a relatively low adsorptivity at high pressures, it surpassed super activated carbon in adsorptivity at lower pressures. It was concluded that zeolite 13X could be utilized in a CaO-CO<sub>2</sub> energy storage system by adsorbing product CO<sub>2</sub> that is released from the dissociation of CaCO<sub>3</sub> at lower temperatures and pressures (where zeolite 13X adsorptivity is superior to that of super activated carbon) and desorbing CO<sub>2</sub> at higher temperature and pressure.

### MgO/H<sub>2</sub>O/Mg(OH)<sub>2</sub> chemical heat pumps

Kato et al. (1996) studied the kinetics of magnesium oxide dehydration and hydration for chemical heat pump (heat amplifier) applications. An equilibrium diagram for the magnesium oxide dehydration and hydration reaction system is shown in Figure A-10. They used MgO with an average particle diameter of 10 μm and measured reaction kinetics using gravimetric analysis. Magnesium hydroxide

dehydration was performed at standard conditions of 623 K and 1.3 kPa prior to the hydration experiments. The researchers noted that experiments performed using a commercial MgO displayed greatly reduced activity, which was attributed to the high-temperature 1100 K processing of the product during manufacturing operations that enhances the sintering of the particles and decreases the number of sites available to the hydration reactions. Experiments were performed to determine  $\text{Mg}(\text{OH})_2$  dehydration and MgO hydration reaction rate temperature and pressure dependence. The researchers concluded that the reactant MgO has four regimes of water reactivity: containment of water as structural water, physical adsorption of water, chemical reaction with water producing  $\text{Mg}(\text{OH})_2$ , and inert with respect to hydration. These water reactivity regimes are illustrated in Figure A-11. Freundlich isotherm was adopted to describe the initial rapid physical adsorption of water onto MgO. The hydration reaction was assumed to have a reaction intermediate  $\text{MgO} \cdot \text{H}_2\text{O}$ . The steady-state approximation and Arrhenius temperature dependence were implemented to determine an apparent rate constant. The ceiling hydration limit is a sorption equilibrium described by a Brunauer adsorption isotherm dependent on hydration temperature and vapor pressure. Numerical calculations using the derived kinetic expression indicated that MgO hydration chemical heat pump performance would compare favorably against competing heat pump systems, with heat output rates of approximately 100–350 W/kg depending on reaction temperature, pressure, and extent.

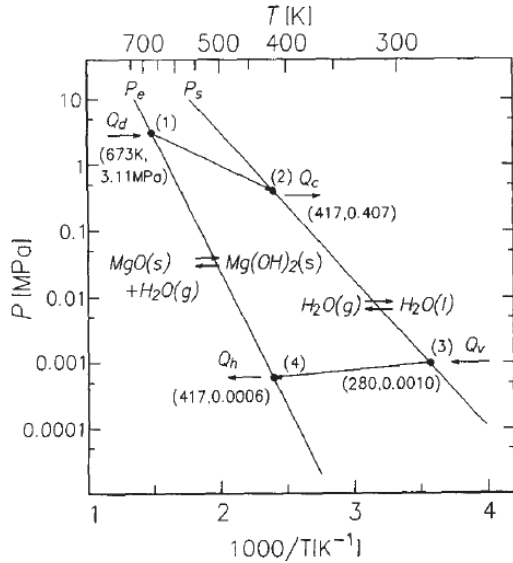


Figure A-10. Equilibrium diagram of the reaction systems of the heat pump.

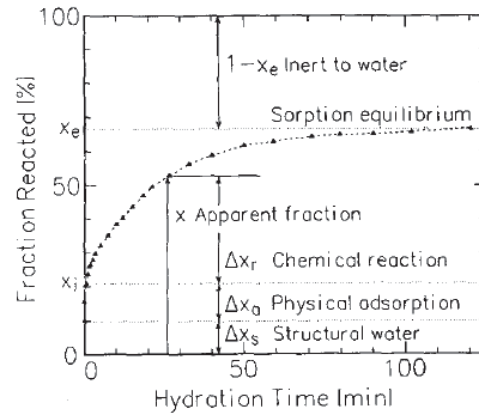


Figure A-11. Schematic diagram of reaction model of the hydration.

Kato et al. (1998) investigated three kinds of magnesium oxide materials in a repetitive hydration-dehydration cycle under reaction conditions representative of a heat storage chemical heat pump to determine which material displayed the best combination of reaction durability and high-heat output performance. Magnesium oxide precursors tested included ultra-fine magnesium oxide powder, common magnesium hydroxide, and magnesium ethoxide. Experiments included repetitive hydration-dehydration reaction cycles ( $T_H = 350^\circ\text{C}$ ,  $T_M = 110^\circ\text{C}$ ,  $T_L = 80^\circ\text{C}$ ) as well as measurement of the material specific surface area by B.E.T. and observations of microscopic structure of the samples using transmission electron microscopy. The ultra-fine magnesium oxide powder exhibited high durability and high-heat output performance relative to the other oxides (Figure A-12). The superior performance of the ultra-fine magnesium oxide powder was attributed to the high purity of the reactant precursors, which resulted in  $\text{Mg}(\text{OH})_2$  samples observed to have a crystallized hexagonal form with a relatively consistent diameter distribution. Following 24 hydration cycles the ultra-fine magnesium oxide powder lost its simple hexagonal crystal form, but retained a similar particle diameter and remained



similarly dispersed. It was concluded that both hydration and dehydration reactions entailed aggregation and cracking of particles, which allows the particle dispersiveness to be maintained at a similar level during repetitive reaction cycles. Following five initial reaction cycles where the reactivity decreased due to structural changes in the primary particles increasing the particle density and vapor diffusion resistance, the reactivity remained relatively constant over the next 19 cycles during which particle cracking provided a fresh reaction surface for each hydration reaction. The heat pump using the ultra-fine magnesium oxide powder output an average of 180 W/kg over the duration of the tests.

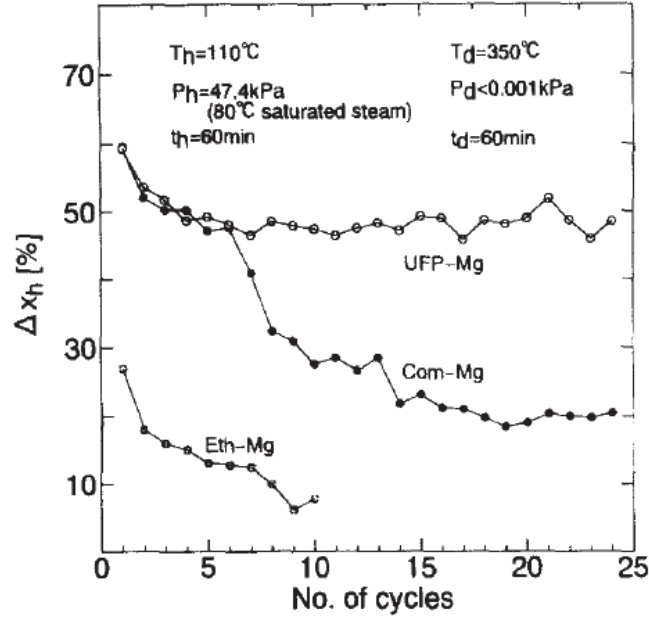


Figure A-12. Reactivity of sample materials in repetitive reactions.

Kato et al. (2000) tested the performance of a packed bed reactor configuration of a  $\text{MgO}/\text{H}_2\text{O}/\text{Mg}(\text{OH})_2$  chemical heat pump to evaluate thermal performance for cogeneration applications. The plate-type packed bed reactor was charged with 1.8 kg of 1.5 mm  $\text{Mg}(\text{OH})_2$  produced from an ultra-fine magnesium oxide powder and water. Heat output mode experiments with temperatures of 110 to 130°C were performed. The experiments indicated that the reacted fraction change and heat recovery ratio increased faster at lower reactor heat output temperatures due to enhancement of exothermic hydration at lower reaction temperatures. In addition, the quantity of heat output recovered increased with lower reactor heat output temperature due to increased exothermic hydration reactivity at lower reaction temperatures. The experimental results are shown in Figure A-13. Analysis of a potential cogeneration system in which diesel engine waste heat was stored by the magnesium oxide chemical heat pump system during periods of low-heat demand and supplied during peak load periods indicated that the heat pump would provide higher heat energy storage density (heat per unit of storage media volume) than a common water sensible heat storage system.

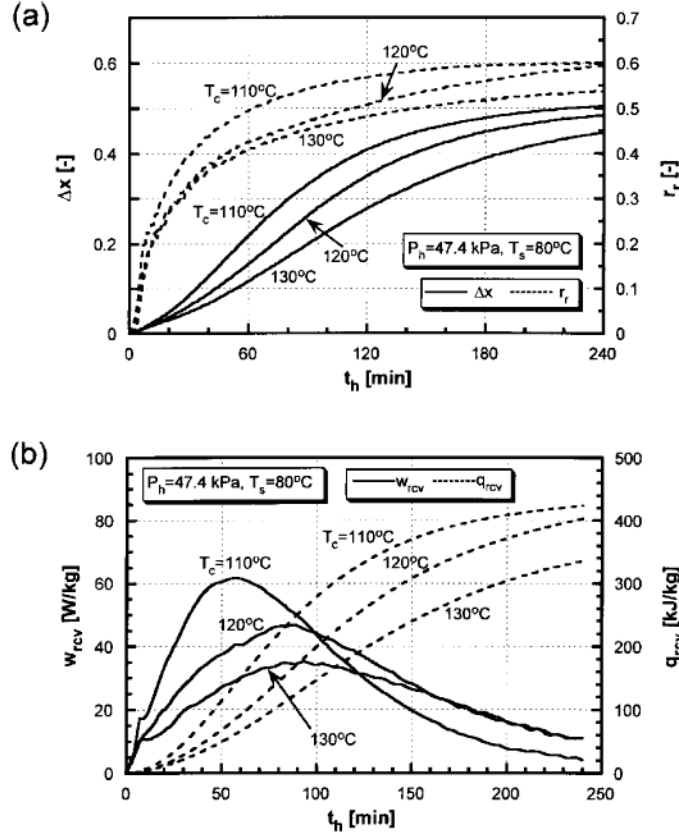


Figure A-13. Effect of heat output temperature on the MgO hydration reactivity: (a) temporal changes in reacted fraction amount and heat recovery ratio, (b) changes in recovered heat output and heat output amount.

Kato et al. (2001) tested the performance of a packed bed reactor configuration of a  $\text{MgO}/\text{H}_2\text{O}/\text{Mg}(\text{OH})_2$  chemical heat pump to evaluate thermal performance for cogeneration applications. The plate-type packed bed reactor was charged with  $\text{Mg}(\text{OH})_2$  produced from an ultra-fine magnesium oxide powder and water. Heat output mode experiments with temperatures of 110 to  $130^\circ\text{C}$  at 47.4 kPa and pressures of 31.2 to 70.1 kPa at  $110^\circ\text{C}$  were performed. The experiments indicated that the reacted fraction change and heat recovery ratio increased faster at lower reactor heat output temperatures due to enhancement of exothermic hydration at lower reaction temperatures. In addition, the quantity of heat output recovered increased with lower reactor heat output temperature due to increased exothermic hydration reactivity at lower reaction temperatures. The reacted fraction change increases faster at higher hydration pressures because the hydration reactivity increases at higher pressures. The heat recovery ratio decreases as the pressures increases because the heat loss from the bed to the inner chamber atmosphere increases with increasing pressure. The experimental results are shown in Figure A-14. The packed bed heat pump reactor was shown to be capable of outputting an average of 100 W/kg at  $110^\circ\text{C}$  for a 54-minute period. Analysis of a combined system in which diesel engine waste heat was stored by the magnesium oxide chemical heat pump system during periods of low-heat demand and supplied during peak load periods indicated that the heat output from the combined system during the peak periods is expected to be several times that of a common cogeneration heat output using an exhaust gas boiler. The analysis indicated that larger the heat source ratios,  $r_s = q_{\text{hydration}}/q_{\text{sensible}}$ , are obtained at lower output temperatures, because as the temperature decreases the hydration activity increases and the sensible heat load decreases relative to hydration heat load.



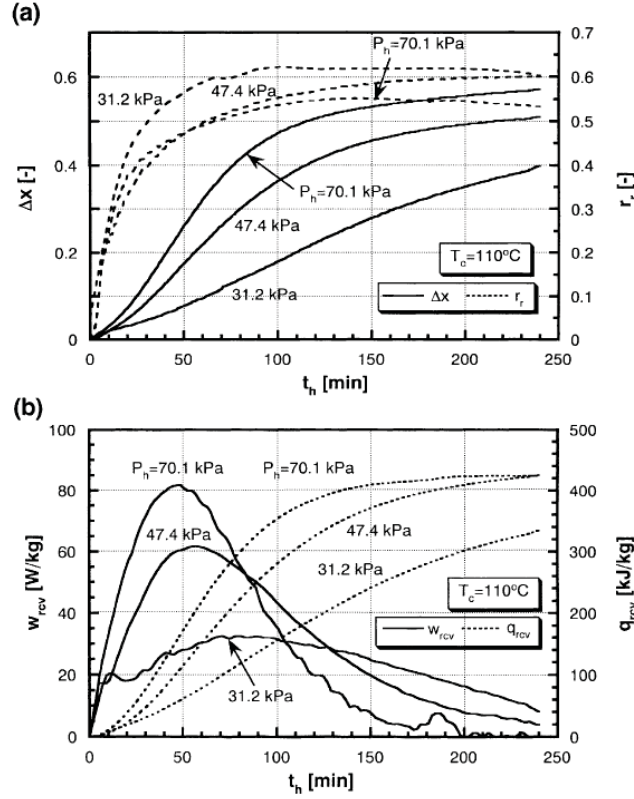


Figure A-14. Effect of hydration pressure on high-temperature output experiment: (a) temporal changes in reacted fraction amount and heat recovery ratio and (b) changes in heat recovery rate and total recovered heat.

Kato et al. (2005) further tested and analyzed the performance characteristics of a  $\text{MgO}/\text{H}_2\text{O}/\text{Mg}(\text{OH})_2$  chemical heat pump for cogeneration heat storage applications using a cylindrical packed bed reactor with thermocouples distributed along the radial and axial dimensions of the reactor. Thermal insulation of the reactor bed was improved over that in the author's previous work. Increased reaction pressures relative to the author's previous work were evaluated. Experimental results indicated that system performance was controlled by heat conduction in the reactor bed. The heat applied to the outside of the reactor bed for driving the dehydration reaction took considerably longer to increase the bed temperature at inner bed locations than outer bed locations (Figure A-15). As a result, the endothermic dehydration reactions proceeded more slowly in the inner region of the reactor bed where the lower temperatures existed. Additionally, heat generated from the hydration reaction was not conducted from the bed as quickly as it was generated, resulting in the temperature of the inner bed region being greater than that of the outer region. As a result, the exothermic hydration reactions proceeded more slowly in the inner region of the reactor bed where the higher temperatures existed (Figure A-16). The effect of the hydration pressure on the reactor bed temperature is shown in Figure A-17. At a pressure of 203 kPa, a 60 minute hydration operation was projected to generate an output rate of 119 W/kg and a gross output of 427 kJ/kg.

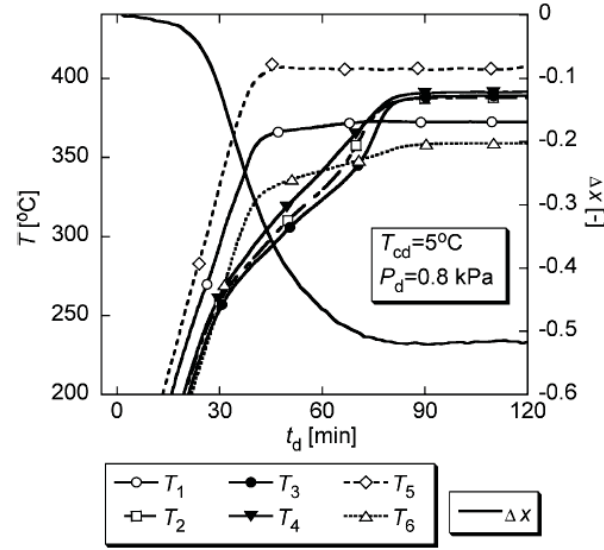


Figure A-15. Bed temperature and reacted fraction profiles for heat storage operation (dehydration of magnesium hydroxide) at  $T_d=410^\circ\text{C}$ ,  $T_{cd}=5^\circ\text{C}$ .

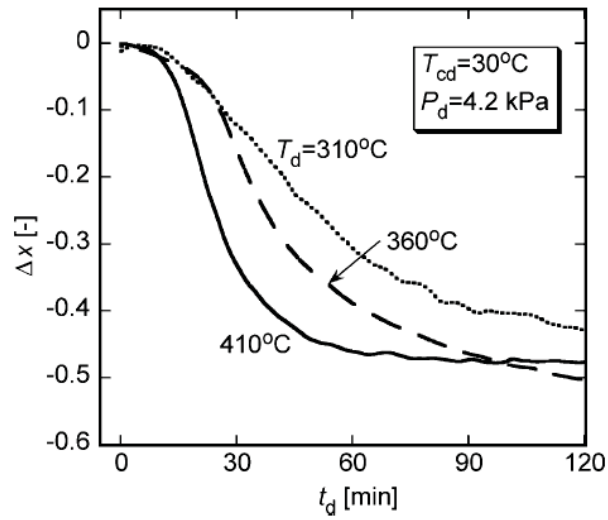


Figure A-16. Effect of dehydration temperature on the reactivity of the reaction at  $T_{cd}=30^\circ\text{C}$ .

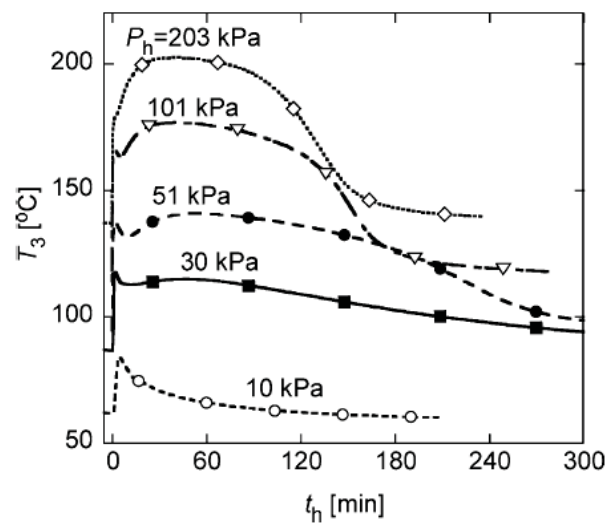


Figure A-17. Effect of hydration pressure on a reactor bed temperature at the bed center  $T_3$ .

## REFERENCES

- Fujimoto, S., E. Bilgen, and H. Ogura, "CaO/Ca(OH)<sub>2</sub> chemical heat pump system," *Energy Conversion and Management*, 43, 947–960, 2002a.
- Fujimoto, S., E. Bilgen, and H. Ogura, "Dynamic simulation of CaO/Ca(OH)<sub>2</sub> chemical heat pump systems," *Exergy*, 2, 6–14, 2002b.
- Kato, Y., K. Kobayashi, and Y. Yoshizawa, "Durability to Repetitive Reaction of Magnesium Oxide/Water Reaction System for a Heat Pump," *Applied Thermal Engineering*, 18(3–4), 85–92, 1998.
- Kato, Y., Y. Sasaki, and Y. Yoshizawa, "Magnesium oxide/water chemical heat pump to enhance energy utilization of a cogeneration system," *Energy*, 30, 2144–2155, 2005.
- Kato, Y., F. Takahashi, A. Watanabe, and Y. Yoshizawa, "Thermal Performance of a Packed Bed Reactor of a Chemical Heat Pump for Cogeneration," *Chemical Engineering Research and Design*, 78(5), 745–748, 2000.
- Kato, Y., F.-u. Takahashi, A. Watanabe, and Y. Yoshizawa, "Thermal analysis of a magnesium oxide/water chemical heat pump for cogeneration," *Applied Thermal Engineering*, 21, 1067–1081, 2001.
- Kato, Y., N. Yamashita, K. Kobayashi, and Y. Yoshizawa, "Kinetic Study of the Hydration of Magnesium Oxide for a Chemical Heat Pump," *Applied Thermal Engineering*, 16(11), 853–862, 1996.
- Kyaw, K., T. Shibata, F. Watanabe, H. Matsuda, and M. Hasatani, "Applicability of Zeolite for CO<sub>2</sub> Storage in a CaO-CO<sub>2</sub> High Temperature Energy Storage System," *Energy Convers Mgmt*, 38(10–13), 1025–1033, 1997.
- Matsuda, H., T. Ishizu, S. K. Lee, and M. Hasatani, "Kinetics study of Ca(OH)<sub>2</sub>/CaO reversible thermochemical reactor for thermal energy storage by means of chemical reaction," *Kagaku Kogaku Ronbunshu*, 11, 542–548, 1985.
- Ogura, H., R. Shimojyo, H. Kage, Y. Matsuno, and A. S. Mujumdar, "Simulation of Hydration/Dehydration of CaO/Ca(OH)<sub>2</sub> Chemical Heat Pump Reactor for Cold/Hot Heat Generation," *Drying Technology*, 17 (7&8), 1579–1592, 1999.
- Ogura, H., H. Ishida, R. Yokooji, H. Kage, Y. Matsuno, and A. S. Mujumdar, "Experimental Studies on a Novel Chemical Heat Pump Dryer using a Gas-Solid Reaction," *Drying Technology*, 19(7), 1461–1477, 2001.
- Ogura, H., T. Yamamoto, H. Kage, Y. Matsuno, and A. S. Mujumdar, "Effects of heat exchange condition on hot air production by a chemical heat pump dryer using CaO/H<sub>2</sub>O/Ca(OH)<sub>2</sub> reaction," *Chemical Engineering Journal*, 86, 3–10, 2002.
- Schaube, F., A. Worner, and H. Muller-Steinhagen, "High Temperature Heat Storage Using Gas-Solid Reactions," 11<sup>th</sup> International Conference on Energy Storage, Stockholm, Sweden, 2009.